

Ultrapotassic Rocks, Carbonatite, and Rare Earth Element Deposit, Mountain Pass, Southern California

By Gordon B. Haxel

Introduction

The Mountain Pass area of southeastern California, just outside the irregular northeast boundary of the East Mojave National Scenic Area (EMNSA) (fig. 4), is notable for three extraordinary geologic phenomena: a geochemically unique carbonatite intrusion, a world-class rare earth element deposit hosted by the carbonatite, and a suite of mafic to silicic ultrapotassic plutonic rocks that are coeval with and presumably genetically related to the carbonatite. Olson and others (1954) described comprehensively the geology, petrography, and mineralogy of the Mountain Pass area and the rare earth element deposit; their work has been summarized in several succeeding articles (Olson and Pray, 1954; Heinrich, 1966; Woyski, 1980; Möller, 1989). Subsequently, rocks at Mountain Pass have been studied by Watson and others (1974), Crow (1984), DeWitt and colleagues (DeWitt, 1987; DeWitt and others, 1987), and Castor (1990, 1991). Several of these investigations are still underway. Despite the considerable petrologic and economic significance of the alkaline rocks at Mountain Pass, no comprehensive geochemical and petrogenetic study has been published to this date (1993).

In this chapter, a brief summary of the geologic setting, physical configuration, and petrography of the ultrapotassic rocks and carbonatite at Mountain Pass is followed by a more detailed examination of the petrochemistry of the ultrapotassic rocks. The limited chemical data available permit descriptive characterization and provisional comparison with other ultrapotassic igneous suites. Primitive ultrapotassic rocks at Mountain Pass contain remarkably high abundances of many incompatible elements. A simple numerical model supports the hypothesis that these igneous rocks were produced by very small degrees of partial melting of highly enriched lithospheric-mantle peridotite. Finally, the geology, geochemistry, and significance of the Mountain Pass rare earth element deposit are summarized.

Geologic Setting

The Middle Proterozoic ultrapotassic rocks and carbonatite of the Mountain Pass area (unit Yg, pl. 1) crop out within an elongate block of crystalline rocks approximately 60 km long that extends from east of Kokoweef Peak, in the northeastern Ivanpah Mountains, north-northwestward to Mesquite Pass, about 4 km north of the EMNSA boundary (fig. 2; see also Hewitt, 1956). This block is composed largely of Early Proterozoic gneisses and pegmatites (Xg), about 1,700 Ma (see section above entitled "Proterozoic Rocks and Their Mineralization;" see also, DeWitt, 1987; Wooden and Miller, 1990). These rocks are intruded by, but unrelated to, the Middle Proterozoic ultrapotassic rocks and carbonatite. This block of Proterozoic rocks is autochthonous, bounded on the west by a thrust fault and a high-angle fault within the Ivanpah Mountains-Clark Mountain area and on the east by an inferred high-angle fault beneath the western Ivanpah Valley (Hewitt, 1956; Burchfiel and Davis, 1971, 1981). The Proterozoic rocks are cut by Tertiary(?) andesite and rhyolite dikes.

The ultrapotassic rocks and carbonatite are restricted to an area extending from approximately 2 km northwest of the Mountain Pass deposit to approximately 9 to 13 km southeast of the deposit. This outcrop belt of ultrapotassic rocks and carbonatite is truncated on the north by a northwest-trending high-angle transverse fault (Olson and others, 1954, pl. 1). To the southeast, the abundance of ultrapotassic rocks and carbonatite decreases gradually toward Mineral Spring.

Configuration, Distribution, and Age Relations of Intrusions

The ultrapotassic silicate igneous rocks at Mountain Pass include shonkinite (melanosyenite), minette (phlogopite lamprophyre), syenite, and granite. These rocks form several hundred thin dikes and seven larger intrusive bodies. The dikes are approximately 0.3 to 10 m wide and as much as 1,100 m long. Most of the larger dikes dip moderately to steeply southwestward. The larger intrusive bodies are ovoid to irregular in map

view and range from 200 to 1,800 m in largest exposed dimension. The largest of these bodies crops out north of the Mountain Pass deposit.

Carbonatite forms about 200 small dikes and one large intrusive body. Most of the carbonatite dikes are approximately 0.3 to 2 m thick and rather variable in orientation. The dikes intrude both Early Proterozoic gneiss and the Middle Proterozoic shonkinite, syenite, and granite. A few of these tabular carbonate bodies could be veins rather than dikes.

The single largest carbonatite body, called the Sulfide Queen carbonatite body (pl. 1), strikes approximately north-south, has a strike length of approximately 700 m, dips about 40° W., and is roughly 70 m thick (Barnum, 1989). Its principal map dimensions are approximately 700 by 200 m. The carbonatite intrusion is irregular, having apophyses extending into the enclosing Early Proterozoic gneiss, satellitic carbonatite intrusions as much as 60 m long along its margin, and inclusions of gneiss and shonkinite as much as 50 m long within the marginal parts of the intrusion.

Carbonatite is considerably less widespread than the ultrapotassic rocks. Most of the carbonatite dikes crop out within a belt that extends approximately 2 km north from the south end of the Sulfide Queen carbonatite body. Only a few small, scattered carbonatite dikes crop out south of Mountain Pass and Interstate 15; most of these dikes are in close proximity to the smaller (nondike) shonkinite intrusions, and some of them parallel shonkinite dikes.

The general intrusive sequence of rock types in the Mountain Pass area is, from oldest to youngest, (1) the main shonkinite bodies, (2) mesosyenite, (3) syenite, (4) quartz syenite, (5) potassic granite, (6) late minette (or shonkinite) dikes, and (7) carbonatite intrusions, including dikes and the Sulfide Queen body. However, at least one late shonkinite dike appears to cut a carbonatite dike (Olson and others, 1954, p. 16; see also Dewitt and others, 1987).

Geochronology and Isotopic Compositions

Lanphere (1964) obtained K–Ar and Rb–Sr ages of 1,380 to 1,440 Ma for biotite from shonkinite at Mountain Pass and calculated a $^{208}\text{Pb}/^{232}\text{Th}$ monazite age of $1,436\pm 71$ Ma using data from Jaffe (1955) and Gottfried and others (1959). DeWitt and others (1987) conducted a comprehensive U–Th–Pb and $^{40}\text{Ar}/^{39}\text{Ar}$ geochronologic study: apatite from the shonkinite has a U–Pb age of $1,410\pm 2$ Ma; phlogopite from the shonkinite and arfvedsonite from the syenite have $^{40}\text{Ar}/^{39}\text{Ar}$ plateau ages of $1,400\pm 8$ and $1,403\pm 7$ Ma, respectively; and monazites from the carbonatite have Th–Pb ages of $1,375\pm 7$ Ma. Bastnaesite and parisite from the carbonatite have complex isotopic systematics that suggest postintrusion migration of Pb. Collectively, these data indicate that the ultrapotassic rocks at Mountain Pass are approximately 1,410 to 1,400 Ma and that the related carbonatite probably was emplaced some 15 to 25 m.y. later.

Unfortunately, the single determination each of Sr and Nd isotopic composition from Mountain Pass are for two different rock types. The carbonatite has a $^{87}\text{Sr}/^{86}\text{Sr}$ ratio of 0.7044 (Powell and others, 1966); presumably this is the initial ratio as the carbonatite has very high Sr content and very low Rb/Sr ratio (<0.001 ; table 1). ϵ_{Nd} for shonkinite from Mountain Pass is -3.5 (for age of 1,400 Ma) (DePaolo and Wasserburg, 1976). Lead and sulfur isotopic compositions of rocks and minerals from Mountain Pass are discussed by Mitchell (1973), Mitchell and Krouse (1971, 1975), DeWitt and others (1987), and Deines (1989). The “extinct” nuclide ^{244}Pu has been reported at a concentration on the order of 10^{-18} g/g in bastnaesite from Mountain Pass (Hoffman and others, 1971).

Petrography

The following summary of the petrography of the ultrapotassic rocks and carbonatite at Mountain Pass is derived mostly from the detailed descriptions provided by Olson and others (1954). The modal progression from shonkinite to syenite involves decrease in color index and concomitant increase in feldspar content; the granites have markedly lower color index and higher quartz content (fig. 5). Given the Mg–rich character of many of the ultrapotassic rocks at Mountain Pass, much of the dark mica probably is phlogopite. In this summary, the general term biotite is used except where phlogopite was specified in the original descriptions.

Shonkinite

The main shonkinite bodies typically consist of medium- to coarse-grained, equigranular, mesocratic to melanocratic shonkinite composed of subequal proportions of grayish-red microcline, green augite, black biotite, and subordinate amphibole. Microperthitic albite is common within the microcline, but separate grains of plagioclase typically constitute only 1 to 3 volume percent of the shonkinite. Other accessory minerals include various combinations of apatite (typically, 2–4 volume percent), iron-titanium oxides, sphene, zircon, epidote, olivine, and, rarely, pseudoleucite(?). Quartz is absent. The pyroxenes are augite and aegirine-augite. Amphiboles are hornblende and (or) sodic amphibole; commonly, both are present. The sodic amphibole is riebeckite and (or) arfvedsonite. Textures are hypidiomorphic-granular or poikilitic, with microcline enclosing biotite, augite, apatite, and other minerals.

Minette Dikes

The late dikes at Mountain Pass are mafic and fine grained, have phlogopite phenocrysts, and can be classified as either shonkinites or minettes (Olson and others, 1954). The latter term is used here to distinguish these late dikes from the main shonkinites, which are earliest in the intrusive sequence. The minettes consist of K-feldspar, phlogopite, augite or aegirine-augite, and hornblende; accessory minerals are quartz (fig. 5), apatite, sphene, iron-titanium oxides, calcite, and fluorite. Phlogopite, the dominant mafic mineral, is present both as phenocrysts and in the groundmass. Some rocks also contain phenocrysts of pyroxene and (or) hornblende. Biotite-rich melanocratic dikes composed largely of phlogopite and aegirine and subordinate or minor feldspar and calcite crop out in one area north of the Mountain Pass rare earth element deposit.

Syenite and Granite

With decreasing pyroxene and biotite content and increasing feldspar and quartz content, shonkinite grades into syenite (fig. 5). Typical syenite contains approximately 80 to 85 volume percent alkali feldspar (orthoclase and (or) microcline, commonly perthitic); less than 10 volume percent each of plagioclase and quartz; and 10 to 15 volume percent each of biotite, amphibole, and, less commonly, augite or aegirine-augite. Common accessory minerals include hematite, apatite, sphene, zircon, rutile, and allanite. Much of the syenite is coarse grained and equigranular; some contains orthoclase phenocrysts. Textures are hypidiomorphic-granular. Mafic, augite- and biotite-rich syenites generally have mafic phenocrysts. In leucosyenite, biotite is the sole mafic mineral. Some syenites contain hornblende; others, sodic amphibole. Late crocidolite (fibrous or asbestiform sodic amphibole) replaces other mafic minerals and also forms veinlets. Quartz syenite, gradational in character between syenite and granite, is petrographically similar to syenite but contains more quartz.

The granites of the Mountain Pass area are fine to coarse grained and commonly have pinkish alkali-feldspar phenocrysts. Most have modal compositions of quartz-poor syenogranite (fig. 5). The plagioclase is quite sodic (An₆). Color index is typically 10 percent or less, distinctly lower than that of the syenite and shonkinite. Mafic minerals are biotite, hornblende, and sodic amphibole. Accessory minerals include iron-titanium oxides, zircon, apatite, sphene, monazite, metamict thorite(?), allanite, epidote, and fluorite.

Carbonatite

Although Olson and others (1954, p. 59–63) recognized the igneous character and origin of the carbonatite at Mountain Pass from regional, field, petrologic, and geochemical evidence, they conservatively referred to it as “carbonate rock.” All subsequent workers have simply treated the carbonatite as an intrusive igneous rock.

One large mass (the Sulfide Queen intrusive body), a number of smaller masses, and many dikes of carbonatite crop out in the Mountain Pass area. The following summary focuses on the Sulfide Queen carbonatite body, which Olson and others (1954; see also, Heinrich, 1966; Woolley and Kempe, 1989) divided into the following three map units (oldest to youngest): ferruginous dolomite carbonatite (beforsite), barite-calcite carbonatite (sövite), and silicified carbonatite. These three types are mutually intergradational, and each has several textural and compositional variants. The following paragraphs describe the principal compositional types.

The dolomite carbonatite is fine grained and consists of dolomite, barite, and monazite, as well as accessory calcite, magnetite, and pyrite. Some rocks also contain the rare earth fluorocarbonate minerals bastnaesite and parisite (table 2). Local additional accessory minerals include thorite(?), apatite, aegirine, and phlogopite.

Barite-calcite carbonatite is the most abundant rock type within the Sulfide Queen body. This sövite consists of 40 to 75 volume percent calcite, 15 to 50 volume percent barite, and 5 to 15 volume percent bastnaesite and (or) parisite. Common accessory minerals include crocidolite, chlorite, phlogopite, apatite, thorite(?), allanite, zircon, galena, hematite, magnetite, and pyrite. The rock typically has a fine-grained groundmass surrounding blocky, subhedral barite phenocrysts 1 to 4 cm wide.

The silicified carbonatite is texturally similar to the barite-calcite carbonatite but has abundant quartz and correspondingly lower calcite content. The silicified carbonatite consists of bastnaesite, barite, and quartz, as well as subordinate or accessory calcite, monazite, hematite and goethite, sericite, galena, and pseudomorphs of hematite after pyrite. Bastnaesite content is as much as 60 volume percent. Quartz forms both euhedral crystals and late chalcedonic veins or layers.

All three types of carbonatite within the Sulfide Queen body are cut by fractures, veins, and shear zones that are coated or filled with crocidolite, chlorite, iron oxides, or other minerals. Supergene minerals include iron oxides, lead or copper carbonate minerals, quartz, and wulfenite.

Fenitization

Fenitization (alkali metasomatism; Heinrich, 1966, chapter 3; McKie, 1966) is widespread in and around the ultrapotassic rocks and carbonatite. Alteration minerals include microcline, albite, riebeckite (including crocidolite), aegirine, chlorite, phlogopite, barite, calcite, iron oxides, sericite, and quartz. Some, perhaps much, of the fenitization is associated with carbonatite intrusions.

Petrochemistry of Ultrapotassic Rocks

Analytical Data

Whole-rock geochemical data for the ultrapotassic rocks and carbonatite at Mountain Pass are limited in quantity and quality. Published and unpublished data from Olson and others (1954), Crow (1984), Lister and Cogger (1986), and J.P. Calzia (written commun., 1992), as well as new data obtained by the author provide a total of 32 analyses. However, both major- and trace-element data are available for only 15 of these samples, and only the four new analyses reported in table 1 include all of the petrologically important trace elements. The previous analyses include reasonably complete and precise data for only four trace elements, Cr, Rb, Ba, and Sr. Most samples have data for Zr or Hf but not both, as well as Nb or Ta but not both. For several geochemical plots, missing values have been estimated on the basis of the assumption that the ratios of Zr/Hf approximately equal to 37 and Nb/Ta approximately equal to 17, which are observed in common types of chondritic, terrestrial, and lunar mafic igneous rocks (Jochum and others, 1986), apply as well to the silicate ultrapotassic suite at Mountain Pass. Given these limitations, petrochemical interpretations of the ultrapotassic rocks at Mountain Pass are necessarily provisional. Petrochemistry of the carbonatite at Mountain Pass is briefly discussed in a later section.

Watson and others (1974) presented, in an abstract, partial mean compositions for 95 major-element analyses of six rock types from Mountain Pass but reported no trace-element data.

Geochemical data for samples from Mountain Pass have been determined by gravimetric wet-chemical methods and wavelength-dispersive X-ray fluorescence spectrometry for major elements and, for trace elements, by energy-dispersive X-ray fluorescence spectrometry, instrumental neutron-activation analysis (INAA), and inductively coupled plasma-atomic emission spectrometry (ICPES) (Crow, 1984; Baedecker, 1987).

The paucity of complete analyses necessitates the use of two complementary indices of fractionation or evolution: Cr content and *mg* number (*mg*, the molar MgO/(MgO+FeO) ratio, calculated with weight percent Fe₂O₃/(Fe₂O₃+FeO) ratio set to 0.2 (Hughes and Hussey, 1976)). Several common acronyms are used in the ensuing discussions of petrology and mineral resources: REE, rare earth elements; LREE, light rare earth elements (La, Ce, Pr, and Nd); HREE, heavy rare earth elements (Tb through Lu); LILE, large-ion-lithophile

elements (K, Ba, Rb, and Cs); and HFSE, high-field-strength elements (Nb, Ta, Zr, Hf, and Ti). Y is commonly included with the HREE. Though not strictly large-ion-lithophile elements, Th and U frequently behave similarly to, and so are generally included with, the LILE. The subscript “cn” designates chondritic-normalized abundances or ratios (normalizing abundances from Nakamura, 1974).

Major-Element Compositions

Normative compositions calculated for the shonkinites and minettes at Mountain Pass frequently contain nepheline or leucite. However modal nepheline has not been reported; Olson and others (1954) found only a single sample possibly containing pseudoleucite; and Crow (1984) found no nepheline or leucite. The shonkinites lack quartz, but the minettes do contain small amounts of quartz, as much as 3 volume percent. The shonkinites and minettes evidently are silica saturated to marginally oversaturated. The normative nepheline and leucite apparently are artifacts of a formalism ill suited to rocks containing 20 to 40 volume percent biotite. Biotite contains both essential Mg and Fe and essential K, whereas the normative calculation scheme inappropriately allocates Mg–Fe and K to separate minerals.

In their molar proportions of alumina and alkalis, the shonkinites, minettes, syenites, and granites at Mountain Pass vary from marginally metaluminous to weakly peralkaline and from potassic to ultrapotassic (fig. 6). Most samples have unusually high molar K_2O/Al_2O_3 ratios, equal to or greater than 0.6; in contrast, common igneous rocks have molar K_2O/Al_2O_3 ratios less than or equal to 0.3. One sample from Mountain Pass, a syenite, is marginally perpotassic.

Ultrapotassic igneous rocks are generally defined as those that have weight percent contents of MgO greater than 3 and K_2O greater than 3, as well as weight percent K_2O/Na_2O ratios greater than 2.5 or 3 (Bergman, 1987; Peccerillo, 1992). According to these criteria, all or nearly all shonkinites, minettes, and syenites at Mountain Pass, which have K_2O/Na_2O ratios of 2.6 to 16, are ultrapotassic. In the standard classification of igneous rocks by silica and total alkali contents (Le Bas and others, 1986), the shonkinites and minettes plot chiefly in the phonotephrite and tephriphonolite fields.

The granites at Mountain Pass are less unusual compositionally than the more mafic rocks. Most of the granites are merely potassic, having K_2O/Na_2O ratios of 1.4 to 3.0. Two samples of altered granite that have excessively high K_2O/Na_2O ratios, greater than 35, are discussed separately below (these samples are omitted from all geochemical diagrams except fig. 9).

The succession from shonkinite through syenite to granite is marked by increase in SiO_2 content from 47 to 71 weight percent, decrease in MgO content from 11 or 12 weight percent to 1 weight percent or less, and decline of *mg* from about 0.8 to about 0.25 (fig. 7). Using the decline in *mg* as an index of progressive evolution, contents of TiO_2 , P_2O_5 (fig. 8A, 8B), FeO^* (total Fe as FeO), and CaO decrease sharply; Na_2O increases markedly; Al_2O_3 increases moderately; and K_2O content is unsystematic. The K_2O/Na_2O ratio decreases sharply with declining *mg* (fig. 8C).

Effects of Fenitization

Most shonkinites, minettes, syenites, and granites at Mountain Pass have weight percent K_2O/Na_2O ratios of about 2 to 11 (fig. 8C). Two granite samples (not plotted on fig. 8C) have very high K_2O/Na_2O ratios, 37 and 45. Such extreme values are not primary but rather a product of subsolidus fenitization. As might be expected, the fenitized granites are moderately enriched in K_2O and strongly depleted in Na_2O relative to unfenitized granites (fig. 9); Fe, Mg, Ca, P, and Mn are moderately depleted; Si, Al, and Ti are little affected. Surprisingly, Ba is not enriched in the fenites. An additional sample, which has a K_2O/Na_2O ratio of about 66, is so strongly fenitized that its prealteration composition and identity are uncertain.

Shonkinites and Minettes as Primary Magmas

Primary, mantle-derived mafic magmas are considered to have *mg* from about 0.65 to 0.80 (Rock, 1991, p. 131–132), although ultrapotassic primary melts may have somewhat higher or lower *mg* (Foley, 1992). Primary magmas also have moderately high Cr (200–500 ppm), Co (25–80 ppm), and Ni (90–700 ppm) contents. The more Mg-rich shonkinites and minettes at Mountain Pass have *mg* equal to 0.72 to 0.82, Cr contents equal to

400 to 700 ppm, Co contents of about 30 to 40 ppm, and Ni contents greater than or equal to 200 ppm, thus equaling or exceeding common criteria for primary magmas.

The shonkinites and minettes that have the highest *mg* and highest Cr and Ni contents may be partially accumulative. As the main shonkinites are, in general, medium-grained plutonic rocks, they probably do not represent strictly liquid compositions but rather were emplaced in the upper crust as mixtures of magma and crystals. The fine-grained minette dikes, which have *mg* of about 0.72, may more closely approximate liquid compositions. Recognition of rocks that have accumulated mafic minerals is problematic in the absence of detailed petrographic information for the analyzed samples. Comparison with a suite of Scottish lamprophyres (Rock and others, 1986) suggests that some shonkinites at Mountain Pass are primary and some, those that have *mg* greater than 0.75, are accumulative (fig. 10).

Abundances of Lithophile Trace Elements

Abundances of Rb, Ba, Sr, and REE are generally greatest in the shonkinites and minettes, where they are generally enriched over MUCC (abundance in mean upper continental crust; Taylor and McLennan, 1985) by factors of 4 to 20. Overall, Ba is the most highly enriched, averaging 6,700 ppm (12×MUCC) in the shonkinites and minettes. Data for Th are available for only four samples (table 1); three of these, a shonkinite, a syenite, and a granite, have extraordinarily high abundances of Th (160–300 ppm, 15–28×MUCC; these elevated Th values, determined by INAA methods, were confirmed by ICPES methods). The shonkinite also has extraordinarily high F content, 1.4 weight percent (table 1).

All of the ultrapotassic rocks have high abundances of LREE but unexceptional abundances of HREE. In the shonkinites and minettes, mean abundances of La and Ce are about 290 and 670 ppm, respectively; both are about 10×MUCC. In contrast, Yb abundances in the shonkinites and minettes are less than 2×MUCC. The shonkinites, minettes, and syenites all have very steep chondrite-normalized REE spectra, typically having La_{cn} contents equal to 600 to 1800, Yb_{cn} contents of about 17, and $(La/Yb)_{cn}$ ratios of about 30 to 60 (fig. 11). Most samples show small negative Eu anomalies, having Eu/Eu^* ratios of about 0.8 (Eu^* is obtained by logarithmic interpolation between Sm and Tb: $Eu^*=10^{(2/3\log(Sm)+1/3\log(Tb))}$). The granites typically have somewhat lower abundances of all REE; steeper REE spectra, having $(La/Yb)_{cn}$ ratios equal to 60 to 80; and shallower negative Eu anomalies, having mean Eu/Eu^* ratios of about 0.9.

Fractional Crystallization of Shonkinite and Syenite

Abundances of Cr decrease from about 400 ppm or more in the primitive, probably primary, shonkinites and minettes at Mountain Pass to as low as about 50 ppm in the syenites (fig. 12). Other highly compatible elements—Co, Ni, and Sc—show comparable progressive depletion. Precipitous decline of highly compatible elements strongly suggests fractional crystallization. For example, if the cumulates are rich in biotite, augite, and iron-titanium oxides, then the bulk distribution coefficient for Cr might be in the range of 5 to 10. Approximately 20 to 40 percent perfect fractional crystallization (Arth, 1976) would then explain the observed decrease in Cr from shonkinite to syenite. Whether or not fractional crystallization of the shonkinite-syenite sequence was accompanied by assimilation of continental crust cannot be determined from the limited trace-element and isotopic data presently available.

Several lithophile trace elements that are incompatible or highly incompatible during fractional crystallization in most igneous suites act compatibly in the ultrapotassic rocks at Mountain Pass, owing to the unusual assemblage of fractionating minerals. For those trace elements that show systematic behavior, most trends can be qualitatively explained in terms of fractionation of minerals present in the rocks. During progressive fractional crystallization (as indicated by declining *mg* and Cr content), Ba and Sr contents decrease (fig. 13) as do P and Ti contents (fig. 8). Progressive depletion of Ba can be explained by fractionation of alkali feldspar and biotite; depletion of Sr, by precipitation of alkali feldspar and apatite. Although Sr depletion is commonly interpreted as evidence of plagioclase fractionation, alkali feldspar also can have a large partition coefficient for Sr (Villemant and others, 1981). Depletion of Ti presumably was caused by fractionation of some combination of biotite, augite, and iron-titanium oxides. Decrease of P indicates apatite fractionation, and the strong correlation between P and Ce (fig. 14A) suggests control of the LREE by apatite crystallization. The

abundance of Rb shows no systematic change with progressive evolution; a preponderance of alkali feldspar and biotite in the fractionating mineral assemblage(s) apparently prevented Rb from behaving incompatibly.

Lithophile trace elements other than those just discussed exhibit less systematic behavior (possibly in part owing to analytical imprecision). Many pairs of trace elements either do not correlate or show weak correlations that are of uncertain significance, given the limitations of the data. Some of these trace elements probably are controlled or affected by several different fractionating minerals. For example, significant amounts of Yb could be hosted by augite, biotite, apatite, sphene, and zircon. Roughly constant Yb contents in the shonkinites, minettes, and syenites (fig. 14B) suggests a bulk distribution coefficient near unity.

Close similarity in the incompatible-element patterns of representative samples of shonkinite and syenite from Mountain Pass clearly evinces their consanguinity (fig. 15). Relative to the parental shonkinite, the derivative syenite shows only slight depletions of Cs, Ba, Th, Sr, and P, all readily attributable to fractionation of observed minerals.

Crow (1984) used major-element and REE data to model the production of syenite from shonkinite by fractional crystallization of an assemblage of aegirine-augite, biotite, apatite, zircon, and minor plagioclase, K-feldspar, quartz, and amphibole. The very small proportion of alkali feldspar in the model precipitate seems to conflict with both the much greater abundance of this mineral in the rocks and the observed depletion of Sr and Ba, which were not considered in the model.

Origin of the Granite

On several trace-element variation diagrams, the granites plot in a separate cluster or trend, distinct from the cluster or trend defined by the shonkinites, minettes, and syenites (for example, figs. 12, 14). This distinction is particularly apparent on plots involving Zr or Yb. Depletion of Zr and HREE in the granites could be explained by the onset of zircon fractionation. However, the shonkinites, syenites, and granites all contain abundant zircon. The presence of discontinuities in several variation diagrams suggests that the granites may not be cogenetic with the shonkinites and syenites. In addition to the possibility of production of the granite by fractional crystallization of syenite or by a separate melting event (Crow, 1984; see also Crow, oral commun., 1987, *quoted by* DeWitt, 1987, p. 54), formation of the granite by assimilation of continental crust during fractional crystallization of the shonkinite-syenite sequence should also be considered.

Whatever their origin, the granites at Mountain Pass are not highly evolved. Highly evolved (highly differentiated) granites are strongly or extremely depleted in the feldspar-compatible elements Sr, Ba, and Eu, having Eu/Eu* ratios of about 0.4 to less than 0.1 (see for example, Mittlefehldt and Miller, 1983). In contrast, the granites at Mountain Pass all have high and roughly similar Sr and Ba abundances, and the mean and least values of Eu/Eu* ratio are only 0.9 and 0.7, respectively.

Shonkinite and Minette: Comparison With Other Ultrapotassic Rocks

The shonkinites and minettes at Mountain Pass have compositions comparable to the most strongly ultrapotassic of terrestrial igneous rocks (fig. 16). All common igneous rock types have weight percent K₂O/Na₂O ratios less than 2. Ultrapotassic rocks, that is rocks that have K₂O/Na₂O ratios greater than 2.5 or 3, make up less than one percent of all igneous rocks; nonetheless, they have received much attention from petrologists. Three widespread petrologic groups of ultrapotassic rocks are recognized: lamproites, kamafugites, and plagioclitites (Bergman, 1987; Foley and others, 1987; Mitchell and Bergman, 1991; Foley, 1992; Peccerillo, 1992). (Kamafugites are strongly silica undersaturated, K- and Ca-rich ultramafic rocks that typically contain kalsilite or melilite. The plagioclitite group includes such rocks as leucite tephrites, leucitites, and leucite phonolites.) Some minettes also are ultrapotassic (Rock, 1987, 1991). Petrologic relations between lamproites and minettes are controversial (Bergman, 1987; Mitchell and Bergman, 1991, p. 405; Rock and others, 1992).

The shonkinites at Mountain Pass differ sharply in major-element composition from both kamafugites and plagioclitites. In particular, the shonkinites have decisively lower CaO and higher SiO₂ contents than kamafugites, as well as decisively lower Al₂O₃ and higher MgO contents than plagioclitites (fig. 17). On the other hand, the shonkinites are compositionally similar to the lamproite group. Important similarities, in addition to ultrapotassic character, include low Al₂O₃, CaO, and Na₂O contents and high to very high

abundances of Ba, Zr, LREE, Th, and F. Of the two general types of lamproites, olivine lamproites and phlogopite lamproites, the shonkinites at Mountain Pass have chemical affinities to the latter (fig. 18).

Despite the numerous similarities of the shonkinites at Mountain Pass to lamproites, several significant differences also exist. The shonkinites contain less Ti and Zr than many lamproites and consequently lack the unusual Ti- and Zr-bearing accessory minerals characteristic of lamproites from such classic localities as Leucite Hills, Wyoming, and West Kimberley, Australia. Some shonkinites at Mountain Pass contain small amounts of plagioclase, which is by definition absent from lamproites in the strict sense. Though their LREE contents are similar to those of lamproites, the shonkinites have greater HREE abundances, and therefore lower La/Yb ratios, than most lamproites. Furthermore, a shonkinite from Mountain Pass has initial $\epsilon_{Nd} = -3.5$ (DePaolo and Wasserburg, 1976), whereas lamproites typically are significantly less radiogenic, having initial $\epsilon_{Nd} = -7.4$ to -26 (Mitchell and Bergman, 1991). (The parameter ϵ_{Nd} is defined as

$$\epsilon_{Nd}(t) = [({}^{143}\text{Nd}/{}^{144}\text{Nd})_{\text{sample}}(t)/({}^{143}\text{Nd}/{}^{144}\text{Nd})_{\text{CHUR}}(t) - 1] \times 10^4,$$

where CHUR stands for “chondritic uniform reservoir” and t represents time.)

In figure 19, the shonkinites at Mountain Pass are compared with compositional fields for lamproites and minettes or, more generally, calcalkaline lamprophyres. In their K_2O contents and $\text{K}_2\text{O}/\text{Al}_2\text{O}_3$ ratios, the shonkinites overlap with the high-K part of the calcalkaline lamprophyre field but are more typical of lamproites (figs. 19A–C). Plots of Sr versus Ba contents and Sm content versus La/Yb ratio discriminate particularly well between minettes and lamproites (figs. 19D, 19E). Abundances of Ba in the shonkinites are in the highest part of the minette range, but typical of lamproites. The La/Yb ratio is within the lowest part of the range of lamproites, and typical of minettes. However, the shonkinites contain substantially more Sm than either typical minettes or most lamproites.

Chondrite-normalized incompatible-element spectra (fig. 20A) further illustrate differences between a representative shonkinite from Mountain Pass and some typical lamproites. Although both rock types share the elevated abundances of LILE that are characteristic of ultrapotassic suites, their patterns show three significant contrasts: (1) In the LILE, the lamproite and shonkinite patterns are antithetical. The lamproites are typically enriched in Ba relative to Cs and Rb and depleted in Th and U relative to Rb and K, whereas the shonkinite is depleted in Ba relative to Cs and Rb and strongly enriched in Th and U relative to all other LILE. Furthermore, the shonkinite has extraordinarily high Th and Cs abundances, approximately an order of magnitude greater than those of the lamproite averages. (2) The shonkinite has lower normalized abundances of all the HFSE than the lamproites have. The prominent troughs at Nb–Ta and Ti in the shonkinite pattern are subdued or absent in the lamproite patterns, and the lamproites contain somewhat more Zr and Hf. (3) The shonkinites have considerably higher HREE and Sm contents than the lamproites. Possible genetic significance of some of these contrasts is discussed in the next section.

In summary, among ultrapotassic rocks the shonkinites at Mountain Pass are more similar to lamproites than to minettes. However, a few significant differences indicate that the shonkinites are best not classified as lamproites. In general, relations between lamproites, which occur as volcanic and subvolcanic rocks, and plutonic ultrapotassic rocks such as shonkinites are poorly understood (Mitchell and Bergman, 1991, p. 17).

Petrogenesis of Shonkinite

“... kimberlite and potassium-rich magmas. Despite their small volume, such melts are of enormous importance.” —*D. McKenzie, 1989*

According to current petrogenetic concepts, the extraordinary composition of the shonkinites at Mountain Pass can be explained only by partial melting of enriched subcontinental lithospheric mantle (Bergman, 1987; Wilson, 1989, chap. 12; Peccerillo, 1992). The primitive, ultrapotassic, strongly LILE- and LREE-enriched character of the shonkinites could not be produced by crustal contamination of basaltic magma. In general, the genesis of mantle-derived alkaline igneous rocks probably involves interaction of both lithospheric and asthenospheric components (Menzies, 1987). However, the distinctively high LILE/HFSE ratios of the

shonkinites, even in comparison with other lithosphere-derived ultrapotassic rocks (for example, fig. 20A), indicates a predominantly or completely lithospheric source.

The shonkinites at Mountain Pass share a key major-element characteristic with the lamproite suite: distinctively lower contents of Al, Ca, and Na than other primitive mafic rocks. This indicates derivation from infertile, refractory, magnesian, harzburgitic peridotite that has been previously depleted in Al, Ca, and Na by extraction of basaltic magma (Mitchell and Bergman, 1991, chap. 10). On the other hand, the very high abundances of incompatible elements in lamproites and in the shonkinites at Mountain Pass requires that their mantle sources were enriched or re-enriched in incompatible elements. Such enrichment, or metasomatism, of lithospheric mantle is a global phenomena and apparently can be caused by migration or infiltration of either silicate magmas or volatile-rich fluids (Menzies and others, 1987). Depleted but re-enriched peridotite evidently constitutes much of the continental lithospheric mantle.

Thus, analogy with the much more thoroughly studied lamproite clan suggests a three-stage history for the origin of the shonkinites at Mountain Pass: depletion of the mantle source, then re-enrichment of the source, and, finally, partial melting to generate the shonkinites (compare with Tainton and McKenzie, 1994). With the limited elemental and isotopic data presently available, only the partial melting stage can be elucidated further. Thus, the high to extreme incompatible-element contents of the shonkinites at Mountain Pass must owe to some combination of source enrichment and small degrees of partial melting. The relative importance of these two factors can be explored by means of a simple numerical model for partial melting.

Batch Partial Melting Model

The batch partial melting model assumes that the liquid is in chemical equilibrium with the melting solid and remains at the site of melting until it escapes or is removed as a “batch” of magma. The behavior of a trace element is idealized as

$$c_1(f) = c_s \frac{1}{D + f(1 - P)},$$

where c_s and c_1 are the concentrations of a trace element in the source and derivative liquid, respectively; f , the mass fraction of melt (degree of partial melting); and D and P , the bulk distribution coefficients in the whole rock and the melting assemblage, respectively (Arth, 1976; Wilson, 1989, chap. 3). For each trace element,

$$D = \sum_i x_i^s k_i \text{ and } P = \sum_i x_i^m k_i$$

where k_i is the solid-liquid partition coefficient for the i th mineral; x_i^s , the mass fraction of the i th mineral in the source rock; and x_i^m , its fraction in the melting assemblage.

I have implemented this model as an interactive, graphic spreadsheet in Microsoft Excel®. Input parameters are the mineral-melt partition coefficients and the composition of the mantle source. The input variables, which can be adjusted to optimize the model, are (1) the mass fractions of the source minerals and the melting minerals and (2) the degree of melting. The model (see fig. 21; table 3) is evaluated by comparison with the best characterized sample of the shonkinite at Mountain Pass (sample EM-1, table 1).

Mineralogy and Composition of the Mantle Source

I have assumed, following the evidence and arguments summarized above, that the shonkinites at Mountain Pass were indeed produced by small degrees of partial melting of highly metasomatized and enriched harzburgite. The metasomatic phases considered are those most commonly found as reservoirs of incompatible elements in xenolithic or xenocrystic samples of enriched mantle peridotite: phlogopite, amphiboles (such as potassian richterite, kaersutite, and pargasite), clinopyroxene, rutile, ilmenite, apatite, and garnet (Menzies and Hawkesworth, 1987). Similar but less familiar minerals, such as potassium-barium titanites, also could be involved (Mitchell and others, 1987; Guo and Green, 1990).

Most analyses of mantle xenoliths, including those from the Southwest, lack data for one or more of the elements, notably Th, that are important in the shonkinites. Therefore, I have used as the model source

composition the geometric mean of analyses of eight highly enriched xenolithic peridotites and pyroxenites from South Africa, Yemen, and Germany (table 3; data from Menzies and others, 1987).

Partition Coefficients

Although most published partition coefficients for Ba in biotite or phlogopite are between 1 and 7, Guo and Green (1990) obtained $k_{\text{phlog}}^{\text{Ba}}$ of about 0.2 to 0.8 for a lamproite composition at upper mantle temperature and pressures; I have used a value of 0.29 (Guo and Green, 1990, p. 91). In turn, the value I selected for $k_{\text{phlog}}^{\text{Rb}}$ is based on the expectation that the smaller and more highly charged Ba^{2+} ion is favored over Rb^{1+} for incorporation into K sites (Henderson, 1982, p. 125).

The pronounced depletion of Nb, Ta, and Ti relative to adjacent elements in the incompatible-element spectrum of the shonkinite (fig. 15A) can be generated from a source lacking these depletions only in the presence of a titanium-bearing phase, probably ilmenite or rutile (Foley and Wheller, 1990). Partition coefficients for Ta in ilmenite, approximately 0.3 to 2, are too low to allow successful modeling of Ta in the shonkinite. I have therefore assumed that the titanium-bearing phase is rutile and so have used $k_{\text{rutile}}^{\text{Ta}}$ and $k_{\text{rutile}}^{\text{Hf}}$ values from Jenner and others (1994). For other elements, few partition coefficients for rutile are available in the literature, so I have used averages (geometric means) of published values for ilmenite, magnetite-ilmenite, iron-titanium oxide, and titanium-magnetite. In reality, the source could contain both rutile and ilmenite.

Other partition coefficients were taken from numerous published sources (see table 3 footnotes). Several poorly known but probably small partition coefficients were set to zero. Partition coefficients for olivine and orthopyroxene were assumed to be zero for all the incompatible elements modeled.

Results: Model Magma

For small degrees of melting ($f < 1$ percent), the composition of the model magma is much more sensitive to the fractions of minerals in the source rock (x_i^s) than to the degree of melting (f) or to the mineral fractions in the melting assemblage (x_i^m). Variations in the mineral fractions in the melting assemblage proved to be quantitatively insignificant, so I have simply assumed that the melting assemblage is entirely phlogopite. Abundances of most elements in the model magma are controlled largely by the mass fractions of phlogopite and amphibole in the source. These two variables are not independent, as the phlogopite and amphibole together must account for the K content of the source rock: $[K_2O]_{\text{source}} = x_{\text{phlog}}^s [K_2O]_{\text{phlog}} + x_{\text{amph}}^s [K_2O]_{\text{amph}}$ (see table 3 footnotes).

The model magma that best matches the shonkinites at Mountain Pass (fig. 21) is generated by approximately 0.01 percent melting of enriched harzburgite that contains 4.9 percent amphibole, 3.4 percent phlogopite, approximately 5 (± 5) percent clinopyroxene, and traces of rutile and apatite (table 3). Clinopyroxene slightly improves the fit for Yb and Sr but is not required. For this optimum source mineralogy, model magmas are quantitatively similar for f values ranging from nearly zero to approximately 0.2 percent; for f values greater than or equal to 0.20 percent, the required high abundances of Th can not be generated from the assumed mantle source material. As the observed and modeled chondrite-normalized abundances in figure 21 vary over nearly four orders of magnitude, agreement between the model magma and shonkinite within a factor of two is satisfactory. The optimum model produces satisfactory results for all elements except Sr and Sm (fig. 21).

The high abundances of Th, Rb, Ba, LREE, and Sm in the shonkinites at Mountain Pass can, as expected, readily be modeled as a consequence of combined source enrichment and very low degree of partial melting. The model further demonstrates that depletion of Ti, Ta, and Nb in the shonkinites could owe to residual rutile. However, these depletions could equally well be an inherited characteristic of the lithospheric-mantle source without the need for a residual titanium phase.

Depletion of Sr relative to adjacent elements (figs. 15, 21) in the shonkinites cannot be modeled successfully. If the amount of amphibole or apatite in the source is increased sufficiently to match the Sr depletion in the shonkinites, abundances of LREE and Sm become much too low. Increasing the partition coefficient for Sr in individual minerals to the maximum reasonable value reduces but does not eliminate the problem. Thus, the melting model suggests that Sr depletion in the shonkinites is inherited from their source.

Moderate underabundance of Nd, Sm, and Tb in the model magma owes to retention of these elements by amphibole and, secondarily, by apatite and clinopyroxene. Increasing the ratio of phlogopite to amphibole in the source improves the fit for the Nd, Sm, and Tb but ruins the fit for LILE, La, and Ce. The abundance of Tb and Yb (representing HREE) in the shonkinites at Mountain Pass can be satisfactorily modeled with amphibole and clinopyroxene in the source, without need for garnet. If garnet rather than amphibole plus clinopyroxene controls Yb and Tb, then no reasonable fit can be achieved for LILE.

Conclusions

The simple batch partial melting model can explain most of the important incompatible-element characteristics of the shonkinites at Mountain Pass but only for a tightly restricted set of input parameters and variables. Thus, the model makes three specific predictions concerning the origin of the shonkinites; (1) the mantle-peridotite source was strongly enriched in highly incompatible elements, having abundances approximately 10 to 40 times greater than chondritic or primitive mantle values (fig. 21; fig. 15 caption); (2) the source peridotite contained residual phlogopite, amphibole, clinopyroxene, rutile, and apatite (or, possibly, similar but less familiar minerals) but not garnet; and (3) the degree of partial melting was low, less than 0.2 percent.

Mantle xenoliths from the Southwest (Wilshire and others, 1988) generally are insufficiently enriched to generate the shonkinites at Mountain Pass even at very low degrees of partial melting. However, the probability that the mantle source for the shonkinites is represented in xenolith collections is slight. The shonkinites at Mountain Pass are regionally unique rocks, very small in volume, that must have originated from rare, anomalously enriched mantle. Such material probably constitutes only a tiny fraction of the lithospheric mantle and, therefore, is unlikely to be sampled by xenolith entrainment. The source enrichment in LILE and LREE inferred from the melting model is consistent with regional geochemical evidence (described in the following section), suggesting that the Mojave lithosphere as a whole is anomalously enriched in Th and LREE.

The preferred melting model, having more amphibole than phlogopite (table 3) and no garnet in the source, also rationalizes some of the differences between the shonkinites at Mountain Pass and the lamproite suite (fig. 20A). Phlogopite is probably more important than amphibole in lamproite genesis (Guo and Green, 1990; Mitchell and Bergman, 1991, chap. 10). Mantle phlogopites apparently have somewhat higher Ba/K ratios than mantle amphiboles (Irving and Frey, 1984). This may partially explain the differing LILE systematics of the shonkinites and lamproites. The optimum melting model for the shonkinites does not require garnet in the source, whereas several comparable melting models for lamproites or similar rocks (for example, Cullers and others, 1985) do invoke garnet. This difference is consistent with the markedly higher Yb content and lower La/Yb ratios (figs. 19E, 20A) of the shonkinites.

As expected, the degree of melting required to generate the shonkinites at Mountain Pass is quite small. The optimum value, f equal to 0.01 percent, is not particularly significant as all values of f less than 0.2 percent yield similar model melts. These results are consistent with the hypothesis that low-viscosity, K-rich melt fractions as small as approximately 0.001 percent will separate from their mantle source (McKenzie, 1985). Such magmas will seldom become voluminous enough to rise to upper-crustal or surface levels, which partially explains the scarcity of ultrapotassic and related rocks.

Thus, the shonkinites at Mountain Pass are rare rocks because their genesis (and perhaps that of the associated carbonatite?) requires the conjunction of two unlikely events: melting of unusually highly enriched lithospheric mantle, and ascent of the magma into the upper crust.

Regional Setting; Related Ultrapotassic Rocks Elsewhere in the Mojave Desert

Ultrapotassic to potassic intrusive rocks that are known or presumed to be approximately 1.4 Ga in age are present at some six localities in a discontinuous chain about 130 km long in southeastern California (Castor and Gleason, 1989; Castor, 1991). Mountain Pass lies near the north end of this discontinuous chain. The only locality other than Mountain Pass that has been described in any detail lies near the south end of this chain: the Barrel Spring pluton, located in the southwestern Piute Mountains 10 to 15 km south of the EMNSA and about

90 km south-southeast of Mountain Pass. This small pluton, about 5 km in largest map dimension, consists of shonkinite, syenite, and alkali granite (Gleason, 1988; Gleason and others, 1988). These rocks are potassic to ultrapotassic and generally have high abundances of LILE and, to a lesser extent, HFSE.

Compared with the ultrapotassic suite at Mountain Pass, the Barrel Spring pluton contains a lesser proportion of shonkinitic or melanocratic rocks and greater proportion of silicic rocks, namely, quartz syenite and K-feldspar porphyry. The Barrel Spring rocks are less strongly potassic: more than 90 percent of the Mountain Pass samples, but only about 40 percent of the Barrel Spring samples, have weight percent K_2O/Na_2O ratios greater than or equal to 2.5 (fig. 22).

Several authors (DeWitt and others, 1987; Gleason, 1988; Castor and Gleason, 1989; Castor, 1991) have pointed out that the Middle Proterozoic ultrapotassic to potassic rocks in southeastern California and the carbonatite at Mountain Pass are coeval with and lie within a 1.4- to 1.5-Ga granitic terrane that encompasses much of the Southwest (Anderson and Bender, 1989). These granitic rocks are characterized by moderate enrichment in a number of lithophile elements, but they generally lack the strong to extreme enrichment in LREE, Ba, Sr, and Th found in the Mountain Pass and Barrel Spring suites. The ultrapotassic rocks in southeastern California and the carbonatite at Mountain Pass presumably are genetically related to the larger 1.4-Ga granitic terrane, but the nature of this relation has not been elucidated.

The Th- and LREE-rich character of the ultrapotassic suite and carbonatite at Mountain Pass and similar or related igneous rocks elsewhere in southeastern California apparently reflects the nature of the Mojave crustal province and its underlying lithospheric mantle. Lead-isotopic data show that the Mojave province has anomalously high time-integrated Th/U ratios, averaging about 7 and ranging as high as 15 for many samples, as opposed to the normal or average crustal value of approximately 4 (Wooden and others, 1988; Wooden and DeWitt, 1991). This elevated Th/U ratio evidently was inherited by the shonkinites and syenites at Mountain Pass, for which Th/U ratio is about 11 (table 1). A further tendency toward enrichment in LREE is suggested by an unusual frequency of occurrences of LREE minerals in the Mojave Desert region of southeastern California, southern Nevada, and northwestern Arizona (Jahns, 1952; Heinrich, 1960; Volborth, 1962; Evans, 1964; Otton and others, 1980; DeWitt and others, 1987; Castor, 1991). The most common of these LREE occurrences is allanite in Early or Early(?) Proterozoic pegmatites.

Among the occurrences of 1.4-Ga ultrapotassic to potassic rocks in southeastern California, associated carbonatite is known only at Mountain Pass. Furthermore, the carbonatite body at Mountain Pass is the only one known in California; and none are known in Nevada or Arizona (Woolley, 1987). The only carbonatites known in Utah are a few small dikes associated with a minette-breccia diatreme, in the southeast corner of the state (McGetchin and Nikhanj, 1973). Except for these minor dikes, the known carbonatites nearest to Mountain Pass are several in Colorado and New Mexico. Isotopic dates of these carbonatites are less than 800 Ma, suggesting that they are unrelated to the Middle Proterozoic carbonatite at Mountain Pass.

Carbonatite

Composition

Both its field relations and its extraordinary composition leave no doubt as to the igneous nature of the carbonatite at Mountain Pass. This is corroborated by experiments conducted by Jones and Wyllie (1983, p. 1,723): "The results from our synthetic rare earth carbonate mixture indicate that the addition of H_2O is all that is required to permit the analogous carbonatite at Mountain Pass, California to exist as a liquid magma at a low pressure and at a temperature near $650^\circ C$." Additional experiments support a magmatic origin for the bastnaesite in the carbonatite at Mountain Pass (Wyllie, 1989).

The only published analysis of the carbonatite at Mountain Pass was determined for use as an international geochemical reference (table 1). The material analyzed was mill-feed ore (crushed carbonatite) comprising bastnaesite with "... considerable baryte-celestine, quartz and/or silicates, iron minerals and various carbonates." (Lister and Cogger, 1986). The carbonatite at Mountain Pass shares several key compositional characteristics of the associated shonkinites and minettes: high *mg* (0.75), K_2O/Na_2O ratio (10.7), K_2O/Al_2O_3 ratio (0.61), and Th content (200 ppm). Abundances of Ba, Sr, and LREE are one to two orders of magnitude

greater in the carbonatite than in the shonkinites and minettes. Other differences include much lower Rb contents and Th/U ratios in the carbonatite. Despite its high K₂O/Na₂O ratio, the carbonatite is not strictly an ultrapotassic rock as it contains only 1.3 weight percent K₂O.

The REE spectrum of the carbonatite shows extraordinary LREE enrichment and LREE–HREE fractionation, having La_{cn} content of about 60,000 and (La/Yb)_{cn} ratio of about 3,000 (fig. 11D). The irregularities in the pattern for REE that have a higher atomic number than Gd probably owe to analytical errors (Lister and Cogger, 1986); some other published carbonatite REE spectra show similar, though less pronounced, irregularities.

Comparison With Other Carbonatites

The carbonatite at Mountain Pass is “one of the most unusual of all carbonatites...” (Heinrich, 1966). A number of characteristics distinguish it from most or all other carbonatites (Möller, 1989; Mariano, 1989a, b):

1. Association with potassic rather than sodic silicate igneous rocks.
2. Absence of feldspathoids in associated silicate rocks (most carbonatites are genetically associated with sodic, silica-undersaturated rocks such as nephelinite and ijolite).
3. Absence of volcanic or subvolcanic rocks.
4. Absence of concentric or ring structure.
5. Low abundance of apatite and magnetite.
6. Absence of Ca–silicate minerals (such as garnet or monticellite).
7. Absence of titanium-niobium minerals (such as pyrochlore or perovskite).
8. Extreme abundance of barite and bastnaesite.
9. Bastnaesite and parisite as primary igneous minerals that cocrystallized with calcite, barite, and dolomite (in other carbonatites, bastnaesite is hydrothermal).
10. Extremely high concentration of LREE (fig. 11D).
11. Lack of enrichment in Nb and Ta.

Several unique compositional characteristics of the carbonatite at Mountain Pass are illustrated by comparison with global averages for carbonatites (Woolley and Kempe, 1989) (fig. 20B). The carbonatite at Mountain Pass is relatively enriched in LREE, Ba, and U by factors of 10 to 30 and depleted in Nb by a factor of 5 to 10. This relative depletion in Nb is further emphasized by interelement ratios:

	<i>Nb/Th</i>	<i>Nb/La</i>	<i>Nb/Ti</i>
Carbonatite at Mountain Pass	0.50	0.0049	0.13
Average calcio-carbonatite	23.	2.0	1.8
Average magnesio-carbonatite	6.1	0.75	0.40

Among all terrestrial igneous rocks, carbonatites have the greatest abundances of LREE and the strongest LREE–HREE fractionation, typically having La_{cn} contents of about 1,000 to 10,000 and (La/Yb)_{cn} ratios of about 100 to 1,000 (Cullers and Graf, 1984; Woolley and Kempe, 1989). Thus, even when compared with other carbonatites, the LREE enrichment and REE fractionation of the carbonatite at Mountain Pass are remarkable: La_{cn} content is about 60,000, and (La/Yb)_{cn} ratio is about 3,000 (fig. 11D).

Constraints on the Origin of the Carbonatite at Mountain Pass

Although the geochemical, mineralogical, and physical uniqueness of the carbonatite at Mountain Pass is well established, the genetic significance of these unique characteristics has not been explored. The origin of the carbonatite at Mountain Pass cannot be determined until more petrologic data are available.

In general, the origin of carbonatites is controversial (Le Bas, 1987; Twyman and Gittins, 1987; Hall, 1987; Gittins, 1989; Kjarsgaard and Hamilton, 1989; Hamilton and others, 1989). Among the key facts to be explained are the frequent association of carbonatites with nephelinitic rocks and the very high concentrations of certain incompatible elements, notably LREE and Nb, in most carbonatites. Three possibilities are commonly entertained (Gittins, 1989): (1) fractionation of mantle-derived “carbonated nephelinite” to produce carbonatite; (2) immiscible

separation of a carbonatitic liquid and a nephelinitic or phonolitic silicate liquid from a mantle-derived parent; and (3) direct melting of carbonate-metasomatized mantle peridotite to produce separate carbonatitic and silicate magmas. The first possibility is implausible, as “carbonated nephelinite” magma apparently does not exist in nature, and it is unlikely that fractional crystallization could generate the high to extreme REE and Nb abundances that generally characterize carbonatites. Applicability of either of the remaining hypotheses to the carbonatite at Mountain Pass is problematic. A valid model for the origin of the carbonatite at Mountain Pass presumably will be exceptional, as the association of this carbonatite with potassic rather than sodic silicate rocks, extraordinarily high content of LREE, and pronounced paucity of Nb are exceptional.

The spatial association of the Sulfide Queen carbonatite intrusion with the largest of the shonkinite-syenite intrusions, as well as the spatial association of some smaller shonkinite and carbonatite intrusions, certainly suggests a genetic link. The association is temporal as well: shonkinite magma evidently was present both before and after carbonatite intrusion, and the two rock types yield similar U–Th–Pb ages (Dewitt and others, 1987). A close genetic link could be compatible with the separation of the carbonatite and shonkinite by liquid immiscibility, or with separate but related genesis of the carbonatitic and shonkinitic magmas in the lithospheric mantle, followed by ascent of the two magmas through the same mantle and crustal passages.

The Mountain Pass Rare Earth Element Deposit

Mineralogy and Composition of Ore

Production of REE at the Mountain Pass deposit is from the Sulfide Queen carbonatite body. Textural relations indicate that REE mineralization is dominantly primary or magmatic; only a small portion is hydrothermal (Mariano, 1989a). Bastnaesite and parisite are the chief ore minerals. Subordinate to rare REE minerals (table 2) in the deposit include allanite, ancylite, cerite (Glass and others, 1958), florencite, hydroxylbastnaesite, monazite, sahamalite (Jaffe and others, 1953), and synchisite (Castor, 1990).

The single published major-element analysis of bastnaesite from Mountain Pass (table 4) is of a mineral separate containing about 5 volume percent quartz and minor barite and carbonate minerals. These impurities presumably account for most or all of the reported Si, Ba, S, Ca, and Mg. The composition of the bastnaesite alone can be estimated by recalculating the analysis after allocating Si to quartz, Ca and Mg to their carbonates, and Ba to barite and carbonate. The resulting composition, $(\text{Ce,La,Pr,Nd})_{1.09}(\text{CO}_3)_{1.00}\text{F}_{0.93}$, differs only slightly from the ideal formula of bastnaesite. This slight deviation could be real or it could, in part, owe to analytical error and (or) incorrect assumptions in the recalculation. Specifically, some Ca in the analysis could occupy Ce sites in bastnaesite, and several minor constituents that are probably present in significant amounts in the bastnaesite and (or) in the impurities, notably Sr and OH^{1-} or H_2O (compare with Evans, 1966, p. 31), were not reported in the analysis.

Bastnaesite from Mountain Pass has extraordinary LREE enrichment and LREE–HREE fractionation: La_{cn} content of about 7×10^5 , Yb_{cn} content of about 20, and $(\text{La}/\text{Yb})_{\text{cn}}$ ratio of about 35,000 (fig. 23). Thus, Yb is enriched over average upper continental crust by a factor of only about 2, whereas La is enriched by a factor of nearly 10^4 . Chondrite normalization, commonly used to display REE data (see for example, figs. 11, 23A), deliberately obscures the even-odd alternation of REE abundances. The actual concentration of REE in bastnaesite from Mountain Pass (fig. 23B) reflects the superposition of two effects: the higher solar system and terrestrial abundances of REE that have even atomic number (such as Ce, Nd) than those that have odd atomic number (La, Pr), and the extreme LREE enrichment of the bastnaesite.

Typical REE ore from Mountain Pass contains approximately 40 volume percent calcite, 25 volume percent barite and (or) celestite, 10 volume percent strontianite, and 12 volume percent bastnaesite (Barnum, 1989). The proportions of individual REE in average ore is such that Ce alone makes up about one-half of the total REE content, and the four lightest REE elements together constitute about 99 percent (table 5).

Reserves and Grade; Pricing

Estimates of proven and probable reserves and grade for ore from Mountain Pass are about 28 million tonnes and 8 to 9 weight percent REE oxides, respectively (table 6). Prices of REE produced from Mountain

Pass range from \$16/kg for the abundant LREE oxides Ce_2O_3 and Nd_2O_3 at relatively low purity (96 percent) to \$1,800/kg for highly purified Eu_2O_3 (table 7). Europium, which constitutes only about 0.1 percent of the ore, is much more costly than any of the other REE produced at Mountain Pass.

Processing

Processing of ore at the Mountain Pass Mine is described by Shaw (1959), Kruesi and Duker (1965), Evans (1966), Johnson (1966), Harrah (1967), Warhol (1980), and Neary and Highley (1984). The entire process emphasizes efficient recovery of Eu, the most valuable of the REE (Barnum, 1989). The carbonatite ore, mined by blasting in an open pit, is crushed to free the REE-bearing mineral grains. Following preflotation treatment by heating, agitation, and conditioning agents, the ore and gangue are separated by froth flotation. Initial flotation concentrates contain about 60 weight percent REE oxides. Additional flotation with an HCl leachant removes Ca and Sr carbonate gangue and liberates CO_2 from the bastnaesite and similar minerals, producing a mixture of REE oxides and fluorides that have grades of 70 to 90 weight percent REE oxide. Some of these intermediate or final REE concentrates produced by flotation are dried and packaged; others undergo further processing to partially or fully separate the individual REE.

The initial step in REE separation is leaching with HCl to convert the trivalent REE to soluble chlorides. The only tetravalent REE, Ce, precipitates as CeO_2 . Separation of the remaining REE is accomplished by solvent extraction, an ion-exchange process involving partitioning of individual REE between two immiscible or only partially miscible liquid phases, the aqueous feed solution of trivalent REE chlorides and an organic solvent that preferentially extracts the heavier REE. The first stage of solvent extraction produces principally high purity La, precipitated and packaged as $\text{La}_2(\text{CO}_3)_3$, and La-rich LREE concentrate, precipitated and packaged as carbonate phases. A second stage of solvent extraction separates, purifies, and recovers oxides of Eu and others of the middle and heavy REE. Some products of solvent extraction at Mountain Pass are shipped to other plants for further purification.

Applications of the Rare Earth Elements: Summary

Designation of the lanthanides as “rare” earth elements owes more to unfamiliarity rather than to true scarcity (Muecke and Möller, 1988). Actually, REE are more abundant in the Earth’s upper crust than many familiar elements. The two most abundant REE, La and Ce, are comparable in upper-crustal concentration to the common metals Ni, Cu, Zn, and Pb. Even the least common REE are about 10 to 100 times more abundant than Ag and Au.

Most applications of REE fall into two broad categories: high-volume industrial uses chiefly as catalysts, in metallurgy, and in the manufacture of glass and ceramics; and low-volume “high technology” uses, such as in phosphors, magnets, and special glasses and ceramics (Neary and Highley, 1984; O’Driscoll, 1988; Preinfalk and Morteani, 1989; Vijayan and others, 1989). The first category uses principally LREE in the form of multielement concentrates and compounds; the second uses mostly HREE, and some LREE, as highly purified separate elements.

Most metallurgical applications of REE employ either mischmetal, a Ce-rich mixture of LREE, or LREE silicides (silicides are binary compounds, commonly nonstoichiometric, of metals and Si; for example, $\text{CeSi}_{\approx 0.5}$, Ce_3Si_2 , CeSi , $\text{CeSi}_{\approx 1.3}$, $\text{CeSi}_{1.7-2.0}$ (Aronsson and others, 1965)). Mischmetal is used in several types of steel, in ductile cast iron, and in some nonferrous alloys, particularly those of Mg and Al. The other major application of mischmetal is in pyrophoric alloys, such as those used to make lighter flints. The two principal catalytic applications of REE are in LREE mixtures used in petroleum-cracking catalysts and as Ce used with Pt, Pd, and Rh in catalytic converters for vehicular-exhaust emission control.

Powders of Ce-rich LREE oxide are widely used for polishing glass. High-purity oxides of several REE have applications in glass manufacture, for decolorizing, as coloring agents, and as ingredients in optical glass to affect or control refractive index, dispersion, optical transmissivity, or ultraviolet absorption. Various REE are used to color ceramic dyes or glazes and to produce ceramics for specialized electronic and refractory applications. In addition, REE-bearing phosphors are used in cathode-ray tubes, X-ray screens, fluorescent lamps, and lasers. One of the most economically important high-technology applications of the REE is the use

of Eu and Y in the red phosphors for color televisions and computer monitors (McColl and Palilla, 1981). “The most important invention in the evolution of Mountain Pass was the commercialization of color television in the mid-1960s.” (Barnum, 1989). Permanent magnets utilizing Sm–Co or Nd–Fe–B compounds or alloys have high field strength and resistance to demagnetization and are stronger and lighter than those made of other materials (Herbst, 1993). These REE-bearing permanent magnets are used chiefly in electrical and electronic assemblies and products, including powerful, light-weight electric motors.

Other, minor technological applications of REE are described by O’Driscoll (1988) and Preinfalk and Morteani (1989). Although technical and industrial innovation over the past three decades has generally increased demand for REE, the opposite can also occur. For example, increasing use of plastic and polycarbonate for eyeglass lenses has reduced the use of Ce as a polishing agent.

Possible future major applications of REE include high-temperature superconductivity and safe storage of hydrogen for use as an energy source (Greenwood and Earnshaw, 1984, p. 46). Hydrogen can be reversibly stored at ambient temperatures and modest pressure as lanthanum-nickel hydride. A potential advantage of REE is their relatively low toxicity (Brown and others, 1990) compared with some other industrial metals. In the future, rechargeable batteries using Ni and Cd, which is highly toxic, may be replaced or supplanted by lanthanum-nickel rechargeable batteries (O’Driscoll, 1990). The REE may also have certain agricultural applications (Brown and others, 1990).

In summary, for some applications a single or a few individual REE are the material of choice despite high cost. This situation is exemplified by Eu as a phosphor in cathode-ray tubes, or Sm and Nd as constituents of permanent magnets. In many other applications, the relatively costly REE compete with less desirable but less expensive alternatives or substitutes. For example, recent innovations have reduced the need for REE in some aspects of ferrous metallurgy (Neary and Highley, 1984).

Mineral Resource Significance of the Mountain Pass Deposit

Until recently, the Mountain Pass deposit was the world’s principal source of LREE. Its reported reserves are approximately 28 million tonnes of REE oxide ore. However, the recently developed Bayan Obo, Mongolia Fe–Nb–REE deposit, which has estimated reserves of 48 million tonnes of ore at grades of 6 percent REE oxides, is now the largest known REE deposit (O’Driscoll, 1988; Mariano, 1989b; Drew and others, 1990). The Bayan Obo deposit is advantageous in its comparatively high contents of Eu and Sm, two of the less abundant but more valuable REE (compare with table 7). In 1986, production of REE from the United States, largely from Mountain Pass, and from China were approximately equal. In 1993, U.S. production was 18,000 tonnes of REE oxide derived from bastnaesite, presumably largely from Mountain Pass; total Chinese production was 22,000 tonnes (Hedrick, 1995). (For comparison, total world production of REE oxides in 1993 was 58,000 tonnes.) Thus, Mountain Pass will no longer solely dominate the world’s LREE supply (unless supply from China were to be disrupted or restricted). Nonetheless, Mountain Pass will continue to be a major source of the light and middle REE for the foreseeable future. [The mineral resource significance of Mountain pass has changed significantly since this report was written, in the early 1990s; for current information see Haxel and others (2002)].

Status of the Mountain Pass Deposit in Mineral-Deposit Models

Numerous unusual geological and geochemical characteristics of the REE deposit at Mountain Pass, summarized above, indicate that it is unique among Earth’s REE deposits. Mountain Pass is apparently the only ore deposit, and certainly the only large deposit, mined solely for its REE content (O’Driscoll, 1988; Castor, 1990). With respect to mineral resources, the most significant features of Mountain Pass are its combination of large reserves and high REE grade (fig. 24) and its absence of Nb enrichment or mineralization. Many or most carbonatite REE deposits contain either accessory Nb minerals, such as pyrochlore or columbite, or major Ti minerals, commonly perovskite or sphene, that bear substantial amounts of Nb (Mariano, 1989a). Except for minor sphene, none of these Nb-bearing minerals has been found in the carbonatite at Mountain Pass. The single analysis of carbonatite from Mountain Pass (Lister and Cogger, 1986) indicates only 100 ppm Nb, whereas typical carbonatite Nb deposits contain 1,400 to 21,000 ppm Nb (Cox and Singer, 1986; Mariano, 1989a). Nb has never been produced from the Mountain Pass deposit.

Until the genesis of the carbonatite at Mountain Pass and its extraordinary LREE mineralization have been elucidated, it cannot be assumed that they have the same origin as other carbonatites. Mountain Pass provisionally should be considered a member, presently the only known member, of a separate mineral-deposit model for LREE-rich, Nb-poor carbonatite having primary bastnaesite mineralization. Inclusion of the Mountain Pass REE deposit in the same model with other carbonatite REE deposits (Cox and Singer, 1986) may distort the mineral resource significance of both types of deposits.

In contrast to the Nb-poor carbonatite, the ultrapotassic rocks at Mountain Pass are moderately enriched in Nb and Ta. However, the limitations of the petrochemical data preclude a detailed assessment. Taking the data at face value, some of the ultrapotassic rocks have 100 to 250 ppm Nb, 4 to 10 times average upper crustal abundance. Niobium contents are greatest in the syenites and granites. Exploration for Nb and (or) Ta presumably would focus on pegmatites or greisen zones associated with granitic plutons (Pollard, 1989a) or on granites that are highly evolved, as indicated by strong depletion in the feldspar-compatible elements Ca, Sr, Ba, and Eu (Pollard, 1989b). All granite bodies of the ultrapotassic suite at Mountain Pass are smaller than about 0.5 km in largest map dimension. Though simple pegmatites are common in the Mountain Pass area, these are Early Proterozoic rocks more than 300 m.y. older than and, therefore, unrelated to the Middle Proterozoic ultrapotassic suite. Olson and others (1954) mention only patches or streaks, a few centimeters to a few meters in size, of Middle Proterozoic pegmatite at a single locality, and they describe no greisenlike alteration. None of the analyzed granites from Mountain Pass is highly evolved geochemically. Thus, none of the available data suggests that the Mountain Pass area is favorable for economically significant Nb and (or) Ta mineralization.

Acknowledgments

Thanks to Ted G. Theodore, David M. Miller, Jenny L. Bronk, Caron S. Jones, Chester T. Wrucke, Clay M. Conway, Paul J. Lamothe, James P. Calzia, James H. Wittke, Ardyth M. Simmons, and Donald A. Singer for assistance with various aspects of this report. Edmund Barnum and John Landreth of Molycorp provided grade and pricing information for the Mountain Pass rare earth deposit. The manuscript was improved by reviews and comments from David A. John, James E. Conrad, and Taryn A. Lindquist.

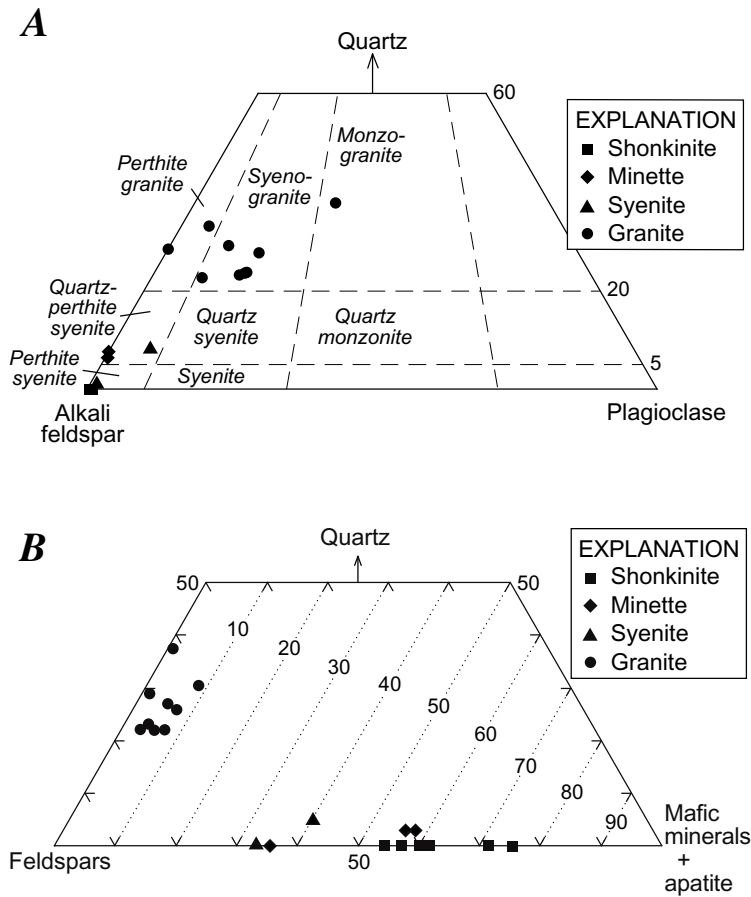


Figure 5. Ternary diagrams of modal composition of ultrapotassic and potassic silicate igneous rocks at Mountain Pass, Calif. (fig. 2). *A*, quartz, alkali feldspar (including perthite), and plagioclase. Seven shonkinite samples and one minette sample plot at or very near the alkali-feldspar apex. Field names and boundaries from Streckeisen (1976). *B*, quartz, feldspars, and total mafic minerals plus apatite; mafic minerals include biotite, augite, amphibole, Fe-Ti oxides, and olivine. Dotted lines show approximate color-index values.

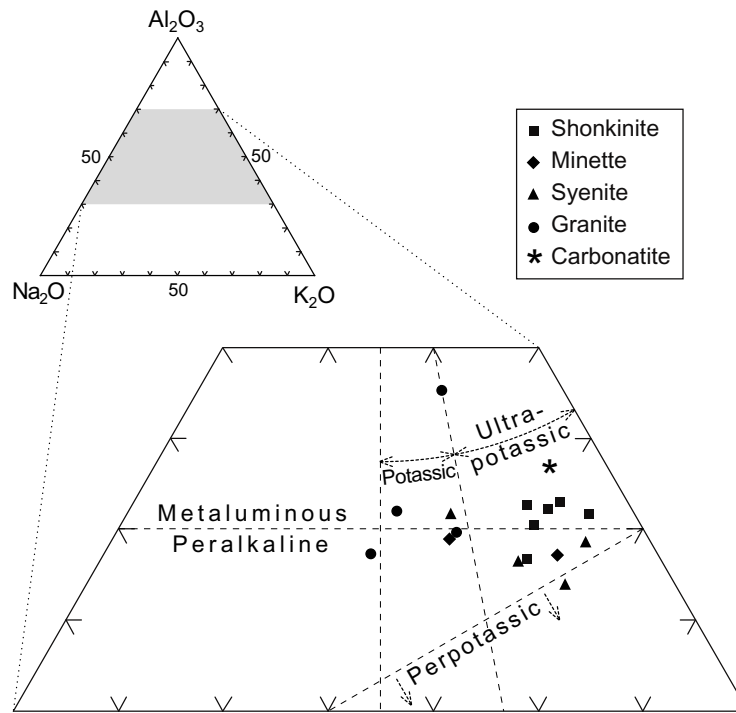


Figure 6. Ternary diagram of molar alumina and alkali content of ultrapotassic and potassic igneous rocks at Mountain Pass, Calif. (fig. 2). Dashed lines distinguish overlapping compositional fields based on the following molar ratios: metaluminous, $(Na_2O+K_2O)/Al_2O_3 < 1$; peralkaline, $(Na_2O+K_2O)/Al_2O_3 > 1$; perpotassic, $K_2O/Al_2O_3 > 1$; potassic, $1 < K_2O/Na_2O < 2$; and ultrapotassic, $K_2O/Na_2O \geq 2$ (equivalent to weight percent $K_2O/Na_2O \geq 3$, the definition of ultrapotassic given by Bergman, 1987).

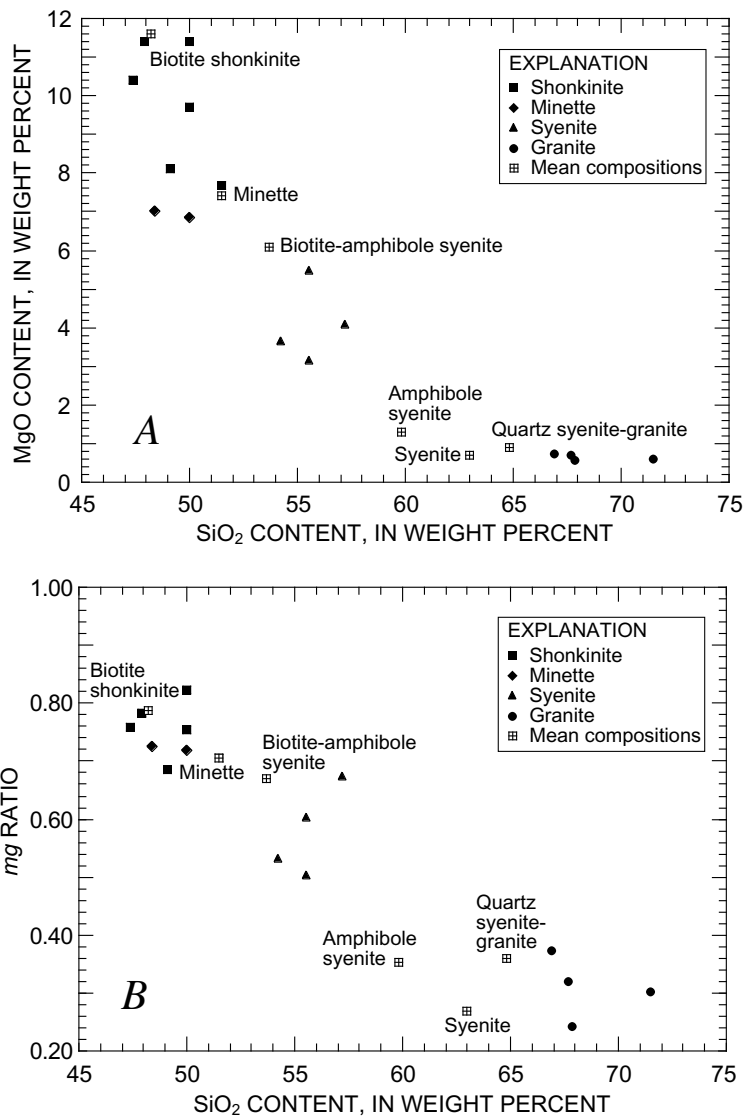


Figure 7. Chemical variation diagrams for ultrapotassic and potassic silicate igneous rocks at Mountain Pass, Calif. (fig. 2). Data for individual samples from table 1, Olson and others (1954), and Crow (1984); mean compositions (labeled with rock type) from Watson and others (1974). *A*, MgO versus SiO₂. *B*, *mg* versus SiO₂; *mg* is molar MgO/(MgO+FeO), assuming weight percent Fe₂O₃/(Fe₂O₃+FeO) = 0.2 (Hughes and Hussey, 1976).

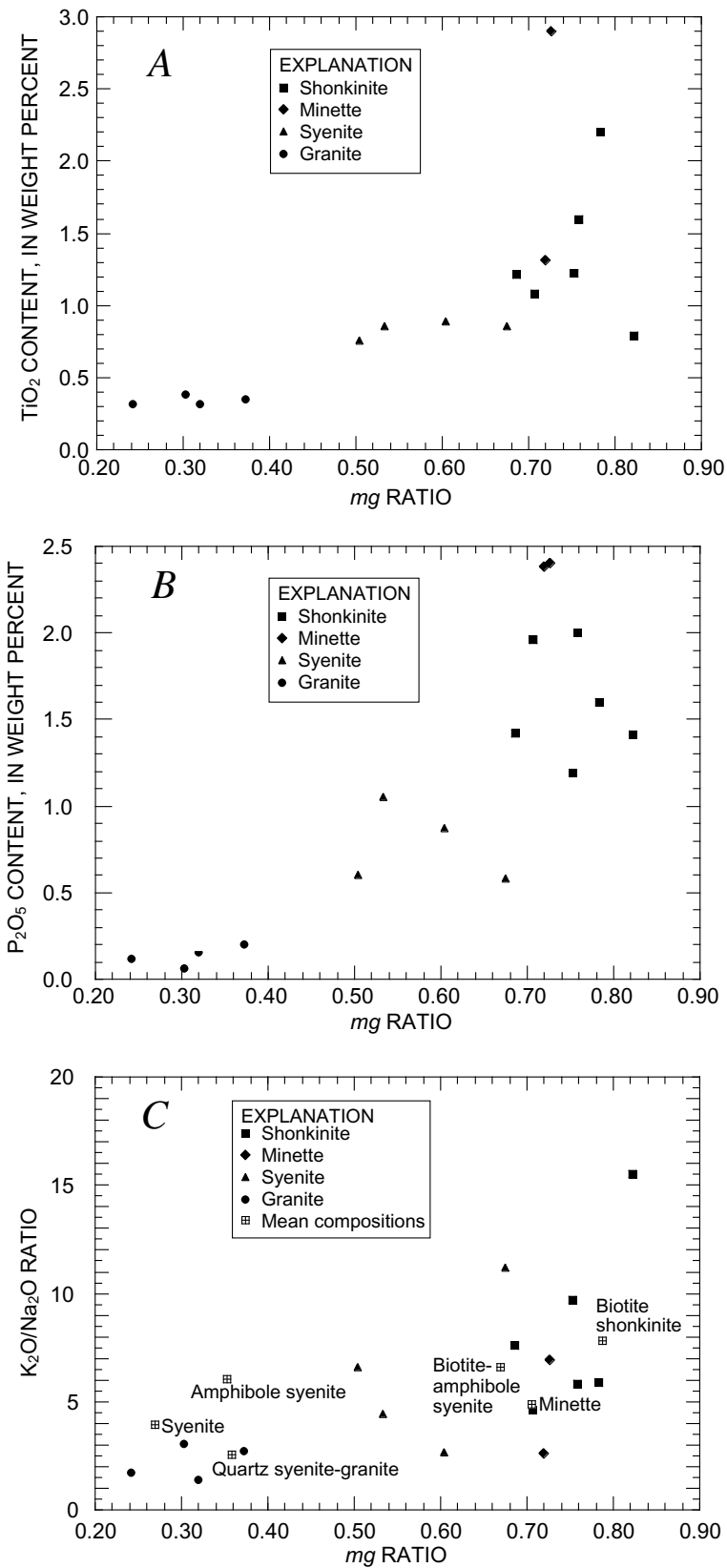


Figure 8. Chemical variation diagrams for ultrapotassic and potassic silicate igneous rocks at Mountain Pass, Calif. (fig. 2), showing decline of TiO₂ and P₂O₅ and K₂O/Na₂O with decreasing *mg* (molar MgO/(MgO+FeO)), assuming weight percent Fe₂O₃/(Fe₂O₃+FeO) = 0.2). Data for individual samples from table 1, Olson and others (1954), and Crow (1984). A, TiO₂ versus *mg*. B, P₂O₅ versus *mg*. C, K₂O/Na₂O versus *mg*; mean compositions (labeled with rock type) from Watson and others (1974).

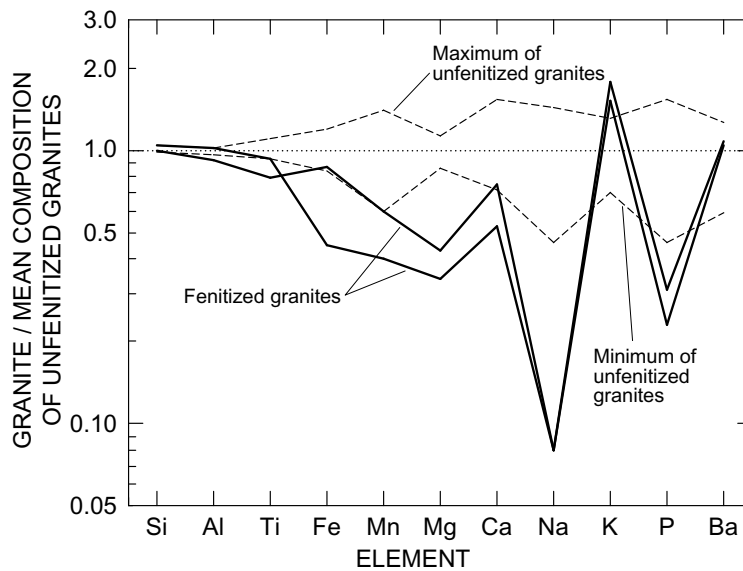


Figure 9. Plot showing major elements and Ba in two fenitized granites (heavy lines) compared with maximum and minimum in four unfenitized granites (dashed lines) from the Mountain Pass area, Calif. (fig. 2). Plotted values are normalized to the mean composition (horizontal dotted line) of the four unfenitized granites.

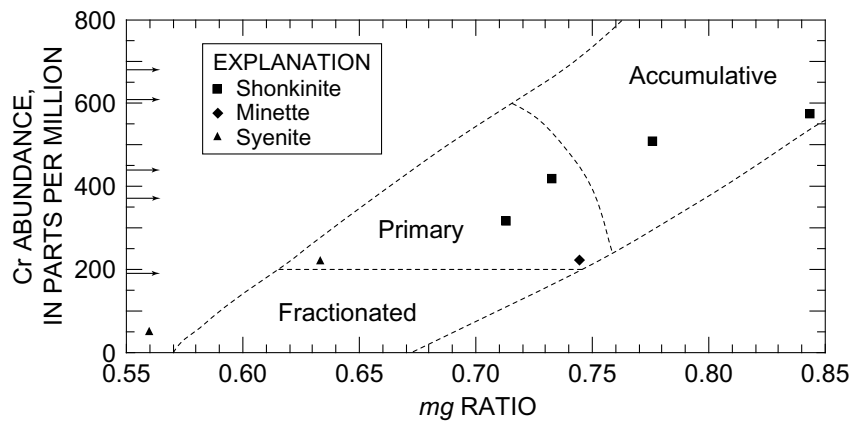


Figure 10. Plot showing Cr versus *mg* in shonkinites, minettes, and two syenites from Mountain Pass, Calif. (fig. 2), compared with the fields of “approximately primary”, accumulative, and fractionated calcalkaline lamprophyres from southern Scotland (diagram from Rock and others, 1986, based on 108 analyzed samples). The lower boundary of the primary field is placed at 200 ppm Cr (Rock, 1991). Arrows along the vertical axis represent Cr content of two shonkinite and three minette samples from Mountain Pass for which major element data are lacking. For this diagram only, *mg* (molar MgO/(MgO+FeO)) is calculated with $Fe_2O_3/(Fe_2O_3+FeO) = 0.3$, for consistency with Rock and others (1986). All syenite samples except the two plotted on this diagram have *mg* < 0.55.

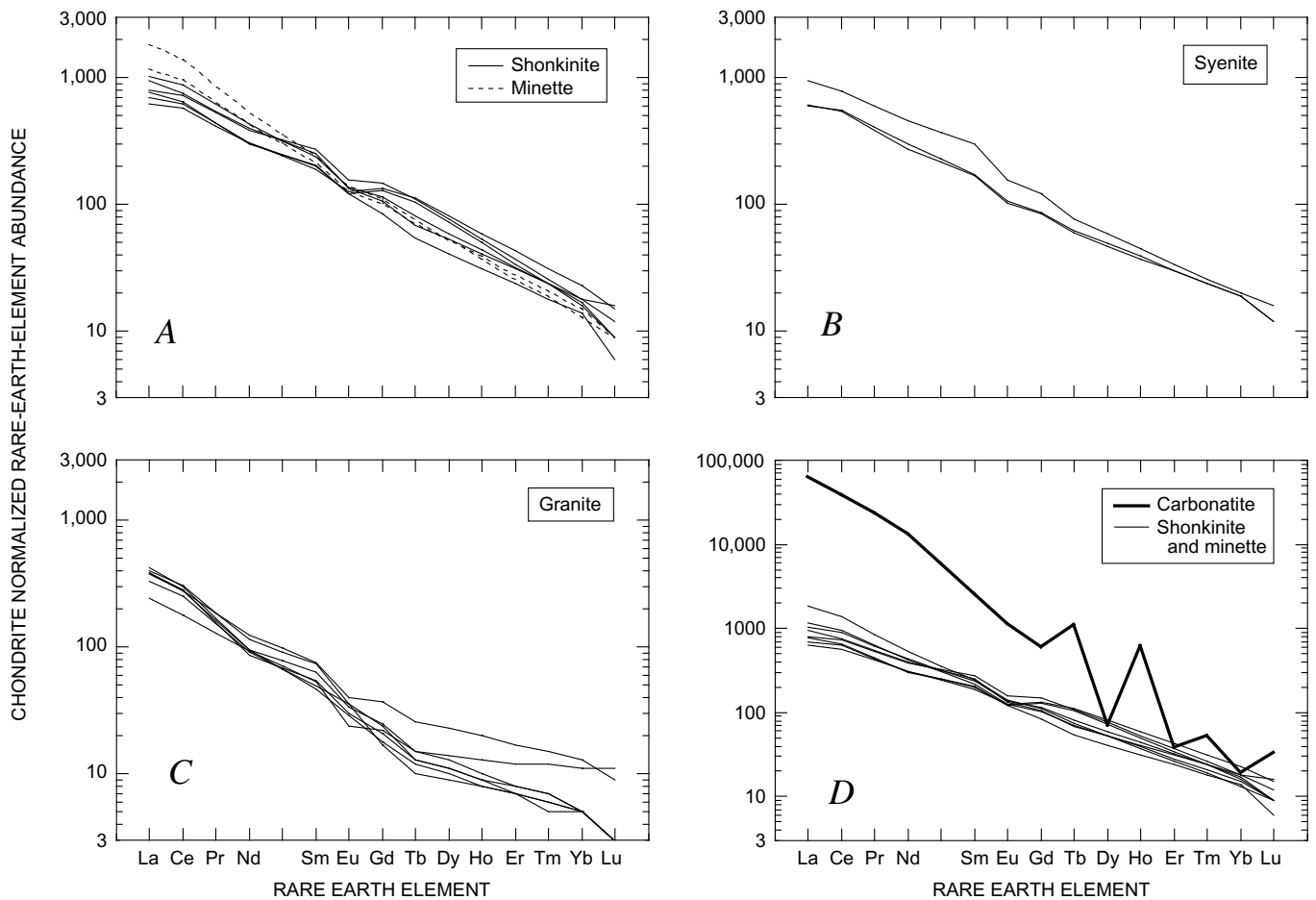


Figure 11. Plots showing chondrite-normalized rare-earth-element (REE) spectra for ultrapotassic and potassic igneous rocks at Mountain Pass, Calif. (fig. 2). Data from table 1, Crow (1984), and Lister and Cogger (1986); normalizing abundances from Nakamura (1974). For 11A, 11B, and 11C, abundances were determined for La, Ce, Nd, Sm, Eu, Tb, Yb, and Lu only; other plotted REE values are interpolated. For 11D, all REE were determined, but values for REE with atomic number greater than Gd may be affected by large analytical errors (see text). A, Shonkinite and minette. B, syenite. C, Granite. D, Carbonatite; REE spectra of shonkinite and minette (from 11A) are repeated for comparison.

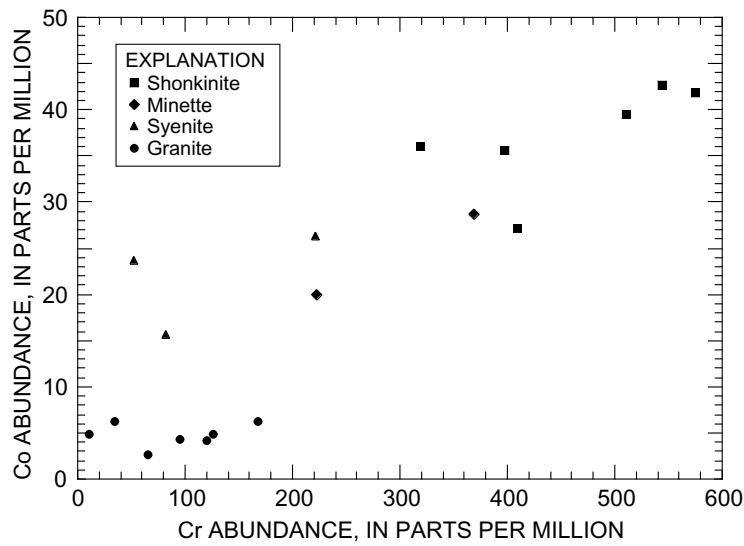


Figure 12. Plot showing covariation of Co and Cr abundances for ultrapotassic and potassic silicate igneous rocks at Mountain Pass, Calif. (fig. 2).

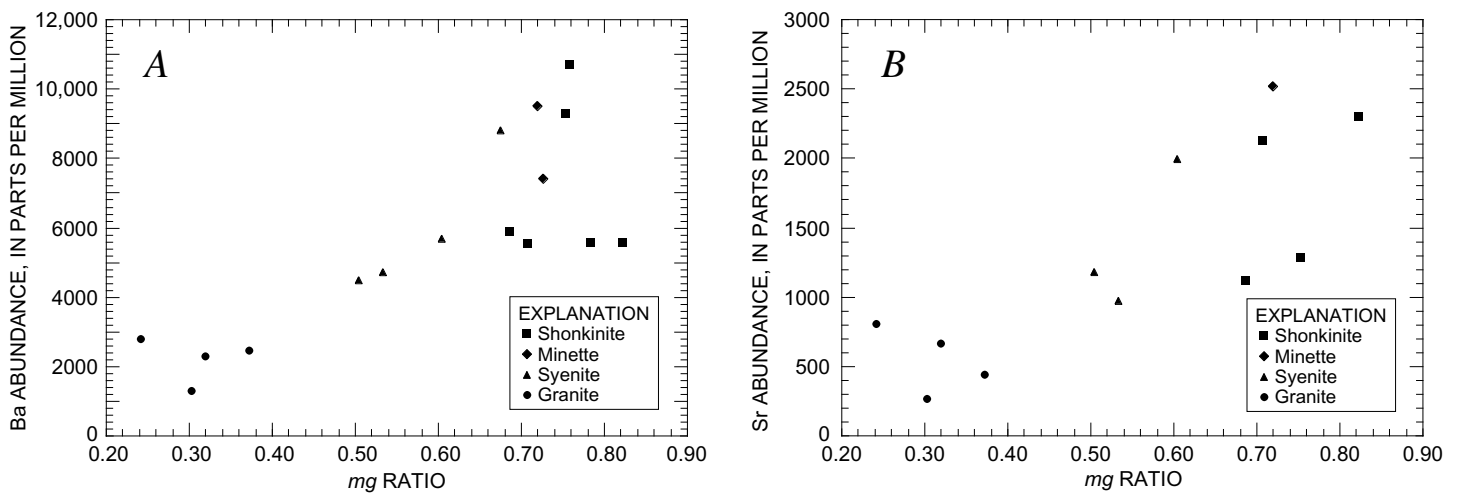


Figure 13. Chemical variation diagrams for ultrapotassic and potassic silicate igneous rocks at Mountain Pass, Calif. (fig. 2), showing the behavior of Ba and Sr during progressive evolution as indexed by the decline of *mg* (molar MgO/(MgO+FeO), assuming weight percent Fe₂O₃/(Fe₂O₃+FeO) = 0.2). A, Ba versus *mg*. B, Sr versus *mg*.

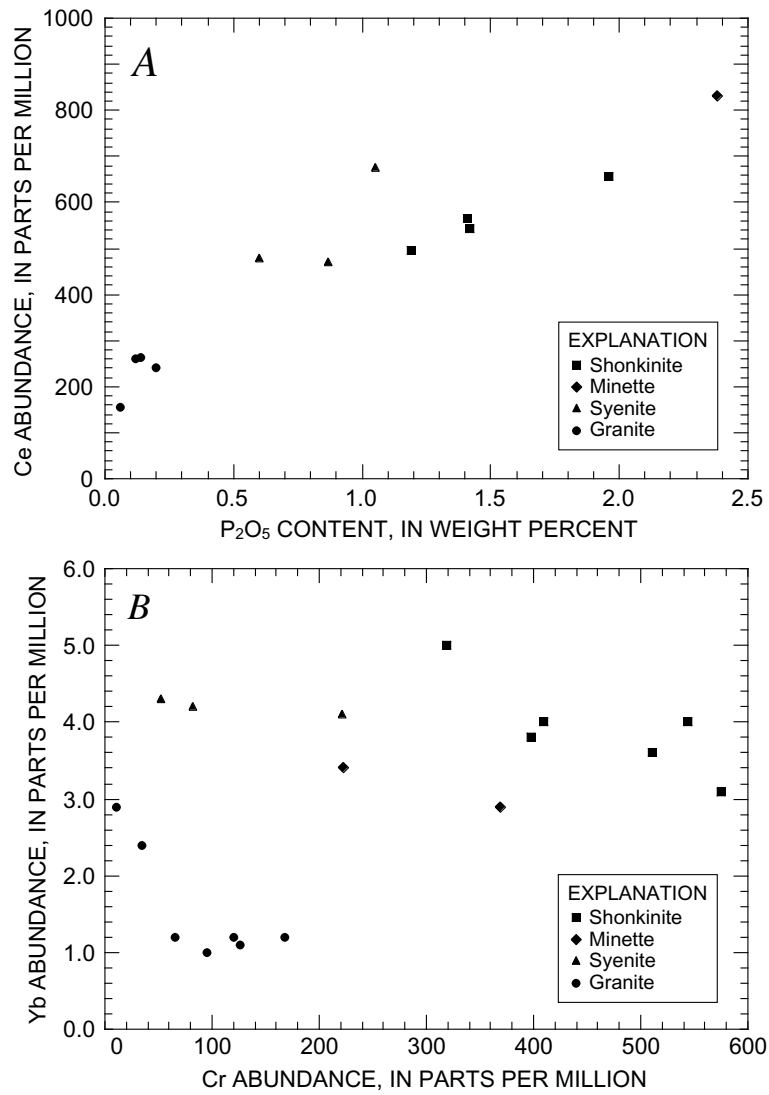


Figure 14. Chemical variation diagrams for ultrapotassic and potassic silicate igneous rocks at Mountain Pass, Calif. (fig. 2). A, Ce versus P₂O₅. B, Yb versus Cr.

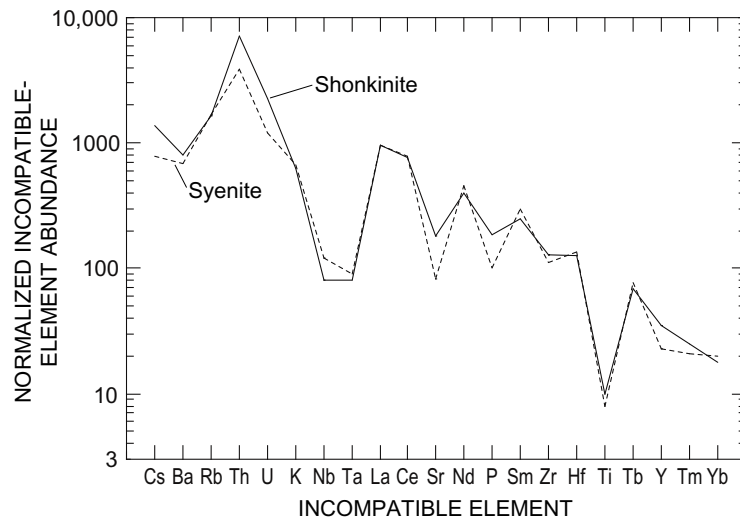


Figure 15. Normalized incompatible-element spectra of two representative ultrapotassic rocks from Mountain Pass, Calif. (fig. 2). The shonkinite (EM-1, table 1) has $mg = 0.71$ and 410 ppm Cr; the syenite (EM-3, table 1) has $mg = 0.53$ and 52 ppm Cr. Normalizing values (R.N. Thompson, 1982a) are chondritic except that values for Cs, Rb, K, and P are estimates for primordial or undepleted terrestrial mantle (Sun, 1980). Normalizing value for U (0.012 ppm) is calculated from the chondritic abundance of Th used by R.N. Thompson (1982a) and the chondritic Th/U ratio of 3.6 (Sun and McDonough, 1989).

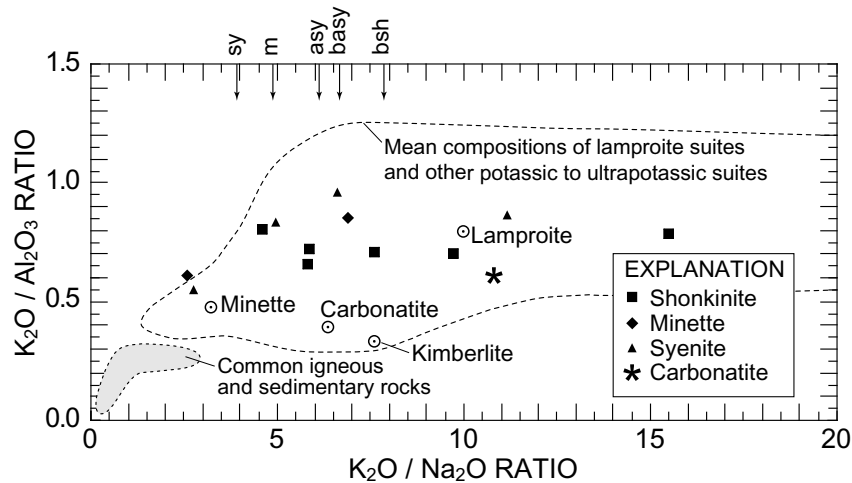


Figure 16. Plot showing weight percent K_2O/Na_2O and K_2O/Al_2O_3 ratios of shonkinite, minette, syenite, and carbonatite at Mountain Pass, Calif. (fig. 2), compared with the field (dashed line) of worldwide mean compositions of lamproite suites and other potassic to ultrapotassic suites (Bergman, 1987). This field extends beyond the right side of the diagram to values of K_2O/Na_2O as large as 50. The global mean compositions of lamproite, minette, carbonatite, and kimberlite are marked by encircled dots. Most Earth materials plot within the small shaded field near the origin. Arrows at the top of the diagram show K_2O/Na_2O for mean compositions of rocks from Mountain Pass (Watson and others, 1974) for which Al_2O_3 content is not given (rock abbreviations: asy, amphibole syenite; basy, biotite-amphibole syenite; bsh, biotite shonkinite; m, minette; sy, syenite).

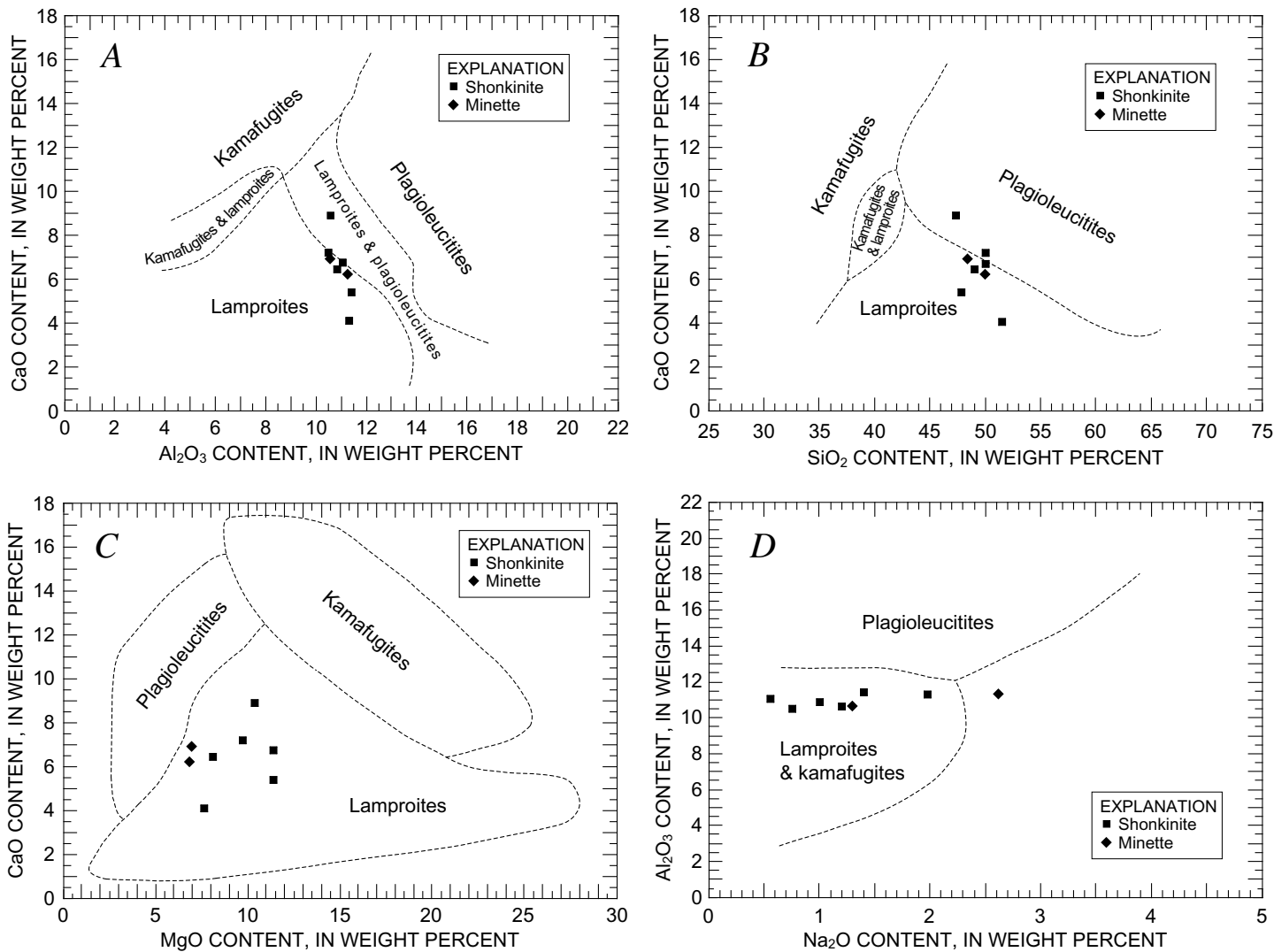


Figure 17. Plots showing abundances of five major oxides in shonkinites and minettes at Mountain Pass, Calif. (fig. 2), compared with generalized compositional fields (dashed lines) of the three major groups of ultrapotassic rocks (after Foley, 1987). A, CaO versus Al₂O₃. B, CaO versus SiO₂. C, CaO versus MgO. D, Al₂O₃ versus Na₂O.

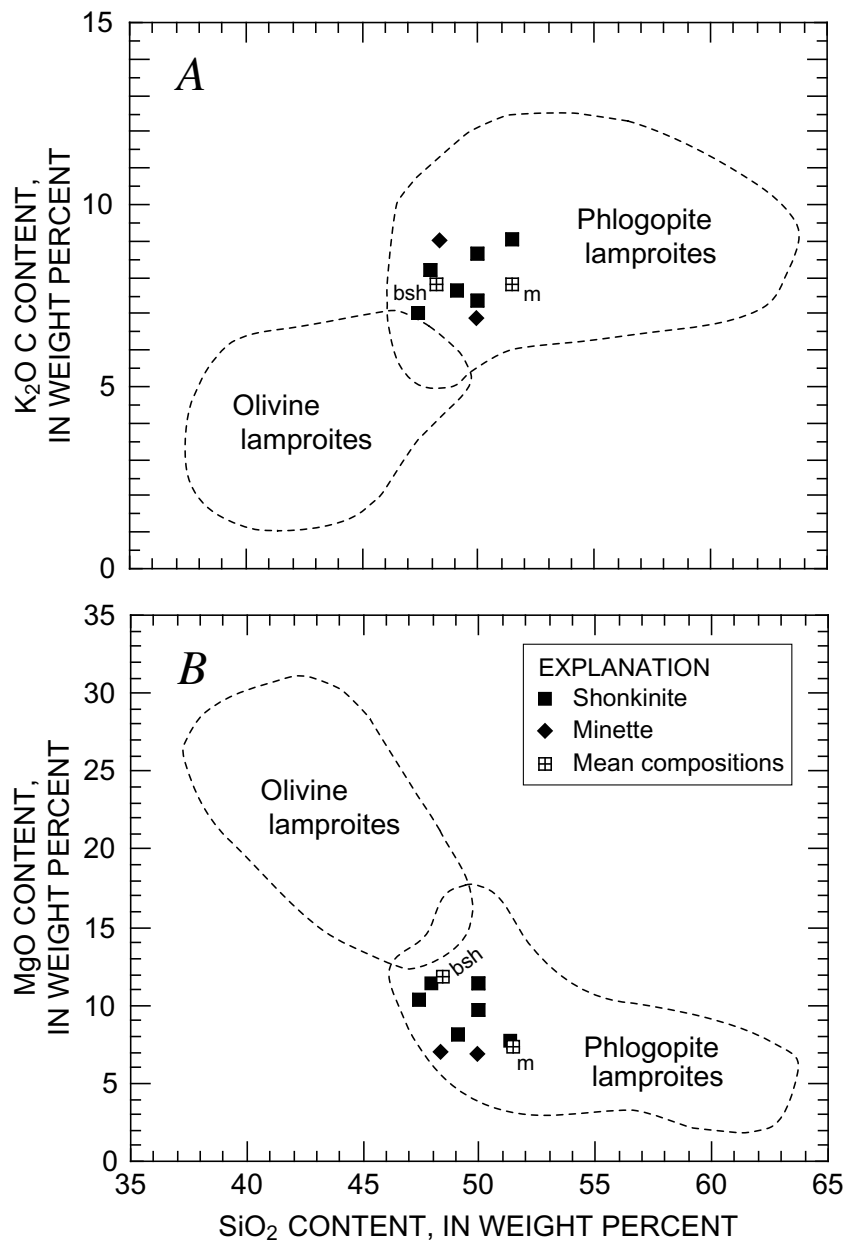


Figure 18. Plots showing SiO₂, MgO, and K₂O (weight percent) in shonkinites and minettes at Mountain Pass, Calif. (fig. 2), compared with compositional fields (dashed lines) of olivine lamproites and phlogopite lamproites from West Kimberley, Australia (from Mitchell and Bergman, 1991, fig. 7.5). Mean compositions of biotite shonkinites (bsh) and minettes (m) at Mountain Pass from Watson and others (1974). *A*, K₂O versus SiO₂. *B*, MgO versus SiO₂.

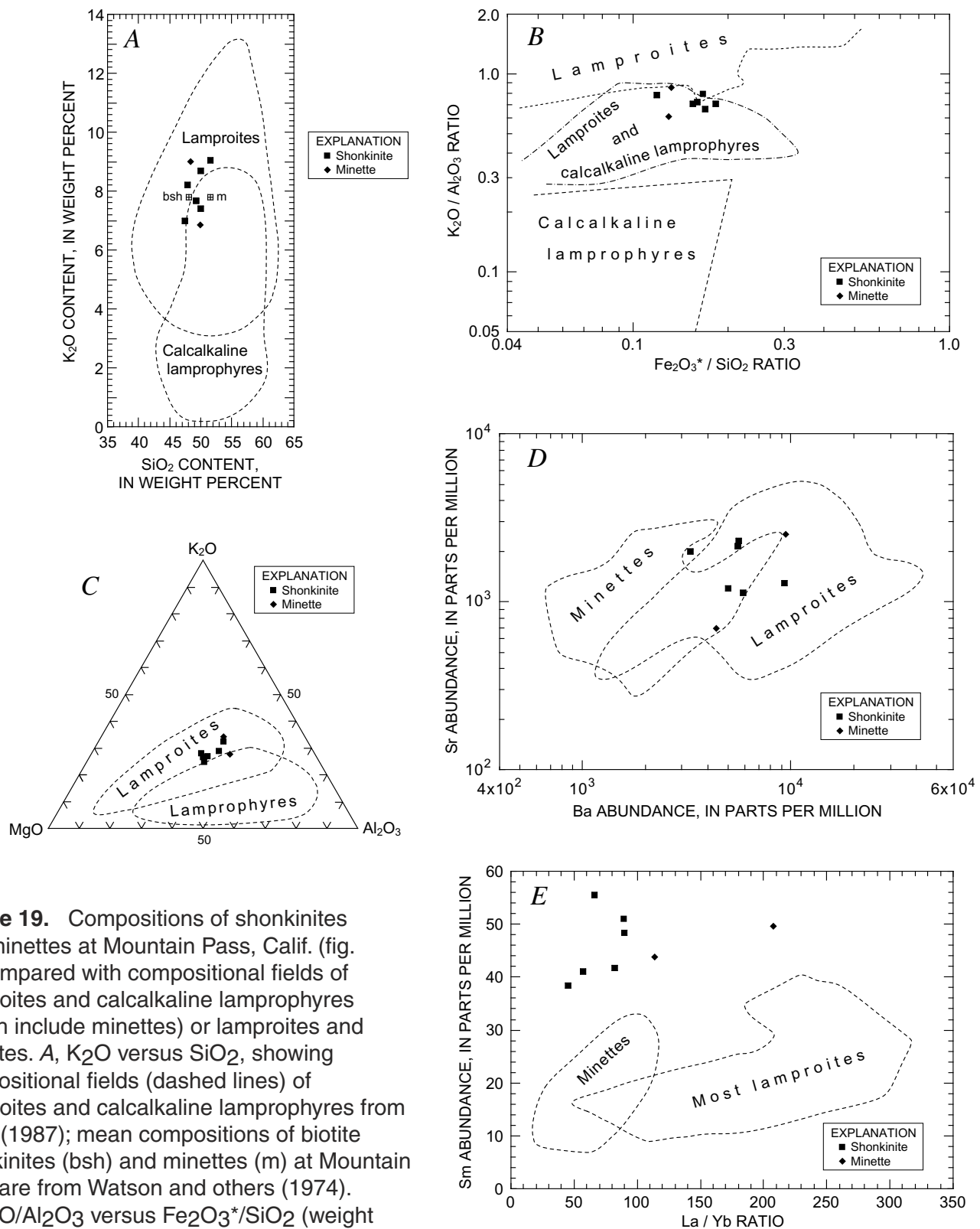


Figure 19. Compositions of shonkinites and minettes at Mountain Pass, Calif. (fig. 2), compared with compositional fields of lamproites and calcalkaline lamprophyres (which include minettes) or lamproites and minettes. *A*, K₂O versus SiO₂, showing compositional fields (dashed lines) of lamproites and calcalkaline lamprophyres from Rock (1987); mean compositions of biotite shonkinites (bsh) and minettes (m) at Mountain Pass are from Watson and others (1974). *B*, K₂O/Al₂O₃ versus Fe₂O₃*/SiO₂ (weight percent); Fe₂O₃* is total iron as Fe₂O₃. Shown are compositional fields (dashed lines) that are diagnostic of lamproites and calcalkaline lamprophyres from Rock (1991, fig. 5.4). Also shown is the field of overlap of lamproite and calcalkaline lamprophyre (dash-dot lines); among hundreds of analyses plotted by Rock (1991), all calcalkaline lamprophyres plot below the upper dash-dot line, and all lamproites plot above the lower dash-dot line. *C*, Ternary diagram of K₂O, MgO, and Al₂O₃ (weight percent) compared with compositional fields (dashed lines) of lamproites and lamprophyres from Bergman (1987). *D*, Sr versus Ba, compared with compositional fields (dashed lines) of minettes and lamproites from Mitchell and Bergman (1991). *E*, Sm versus La/Yb, compared with compositional fields (dashed lines) of minettes and lamproites from Mitchell and Bergman (1991).

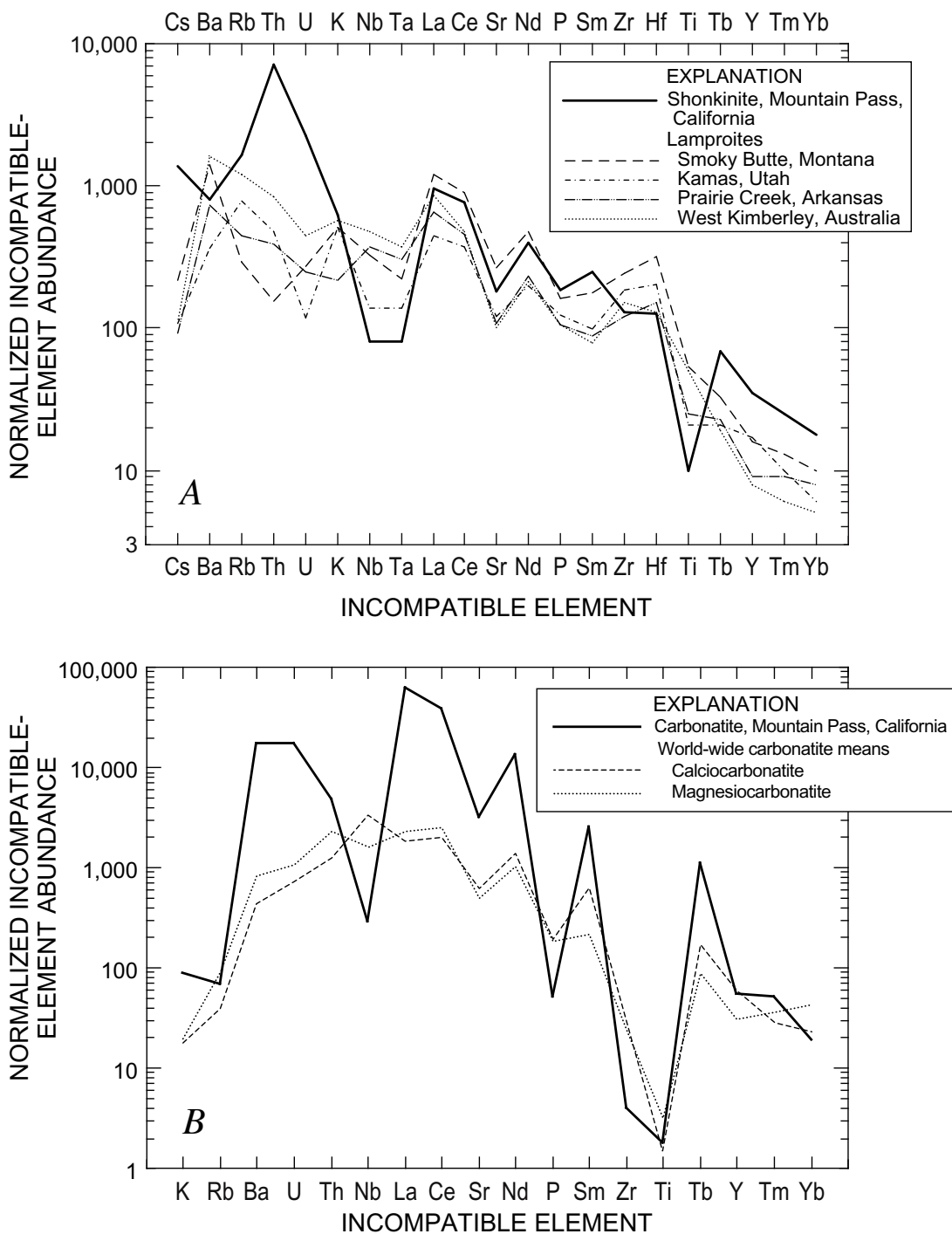


Figure 20. Normalized incompatible-element spectra of two representative alkaline rocks from Mountain Pass, Calif. (fig. 2). Normalizing values (R.N. Thompson, 1982a) are chondritic except that values for Cs, Rb, K, and P are estimates for primordial or undepleted terrestrial mantle (Sun, 1980). Normalizing value for U (0.012 ppm) is calculated from the chondritic abundance of Th used by R.N. Thompson (1982a) and the chondritic Th/U ratio of 3.6 (Sun and McDonough, 1989). *A*, Spectrum of shonkinite (EM-1, table 1) compared with mean compositions of four lamproite suites (Bergman, 1987, table 6; Mitchell and Bergman, 1991, p. 340, 342). *B*, Spectrum of carbonatite (IGS-40, table 1; from Lister and Cogger, 1986), compared with average compositions of calciocarbonatites and magnesiocarbonatites (Woolley and Kempe, 1989, table 1.1). Abundance of Zr in the carbonatite sample, which was not reported by Lister and Cogger (1986), was estimated from Olson and others (1954, table 5).

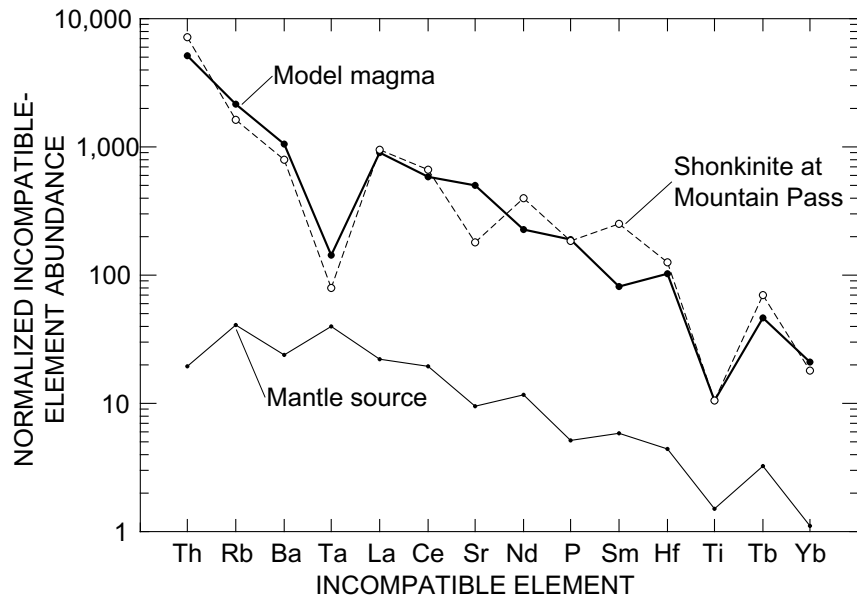


Figure 21. Normalized incompatible-element spectra of assumed mantle source and model magma for preferred batch partial melting model (table 3). Spectrum of shonkinite at Mountain Pass, Calif. (fig. 2; EM-1, table 1) is shown for comparison with the model magma. Normalizing values (R.N. Thompson, 1982a) are chondritic except that values for Rb and P are estimates for primordial or undepleted terrestrial mantle.

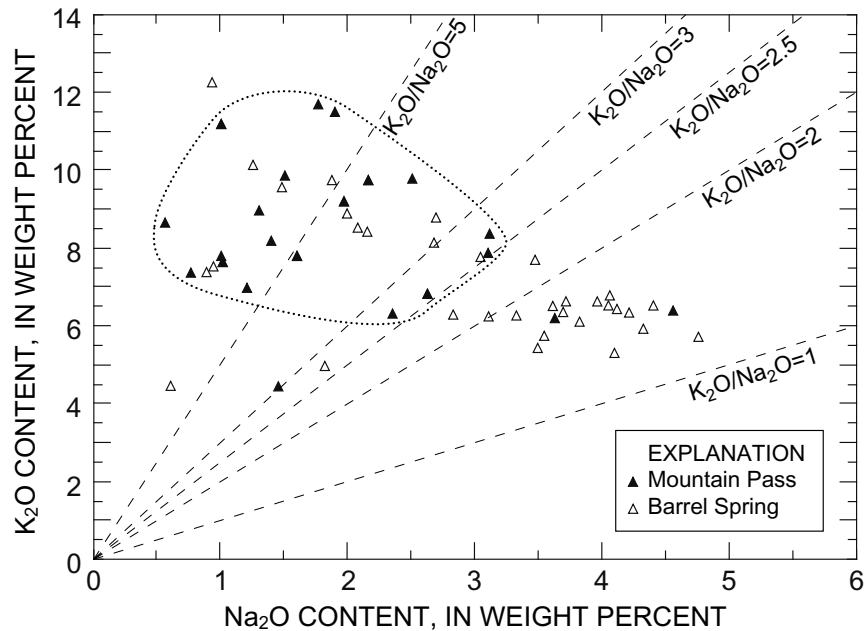


Figure 22. Plot comparing K_2O and Na_2O in ultrapotassic and potassic rocks at Mountain Pass, Calif., and from the Barrel Spring pluton, Piute Mountains, Calif., (fig. 2; Gleason, 1988). Data for Mountain Pass includes both individual samples (data from table 1; Olson and others, 1954; and Crow, 1984) and mean compositions reported by Watson and others (1974). Dotted line encloses compositional field for 86 percent of the Mountain Pass samples and means; three granite samples plot outside this field.

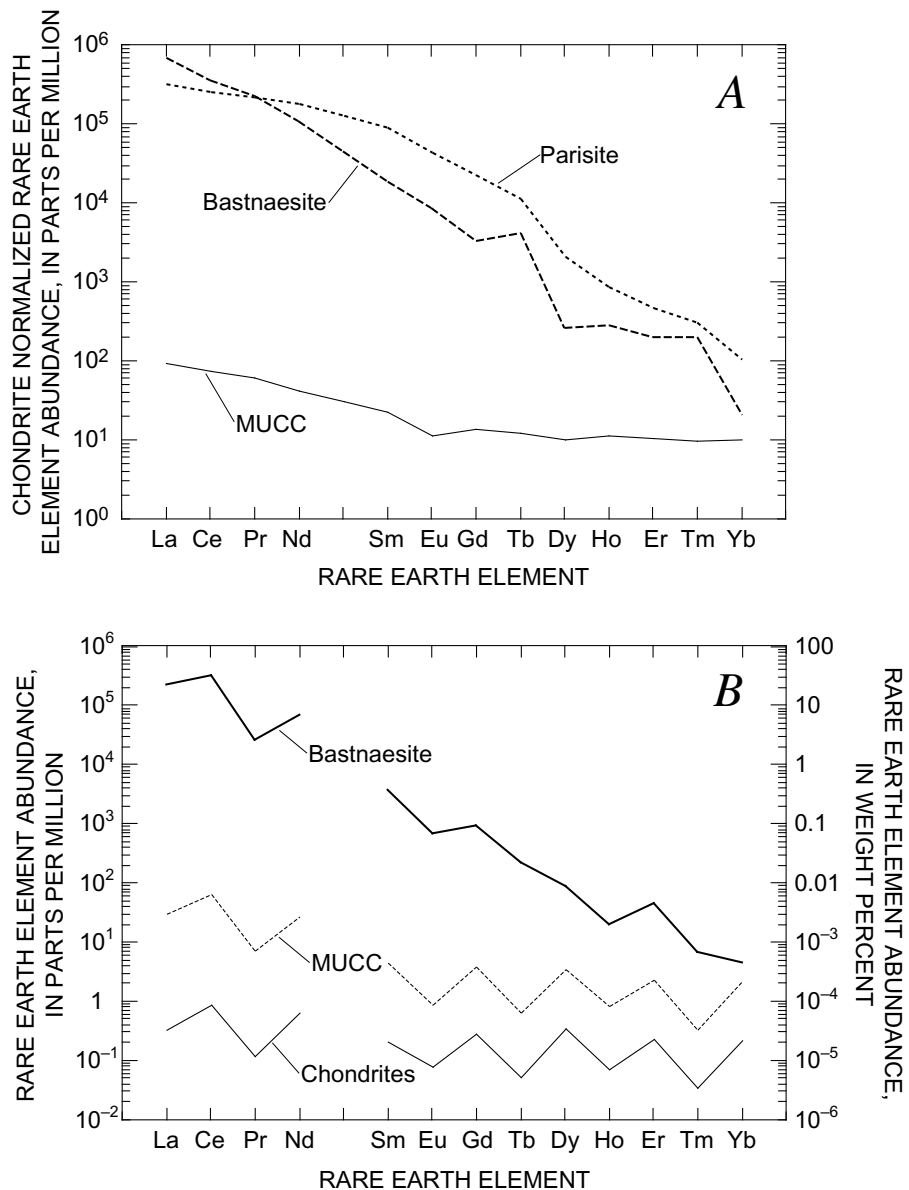


Figure 23. Rare-earth-element (REE) spectra for bastnaesite and parisite from carbonatite at Mountain Pass, Calif. (fig. 2). A, Chondrite-normalized REE spectra of bastnaesite from the Mountain Pass REE deposit and parisite from a carbonatite dike south of the deposit (from Mariano, 1989b; source of chondritic normalizing abundances not specified) compared with Ree spectra of average upper continental crust (MUCC) (Taylor and McLennan, 1985). B, Plot showing REE content, in both parts per million and weight percent, of bastnaesite from the Mountain Pass REE deposit, compared with that of MUCC and CI chondrites (Nakamura, 1974).

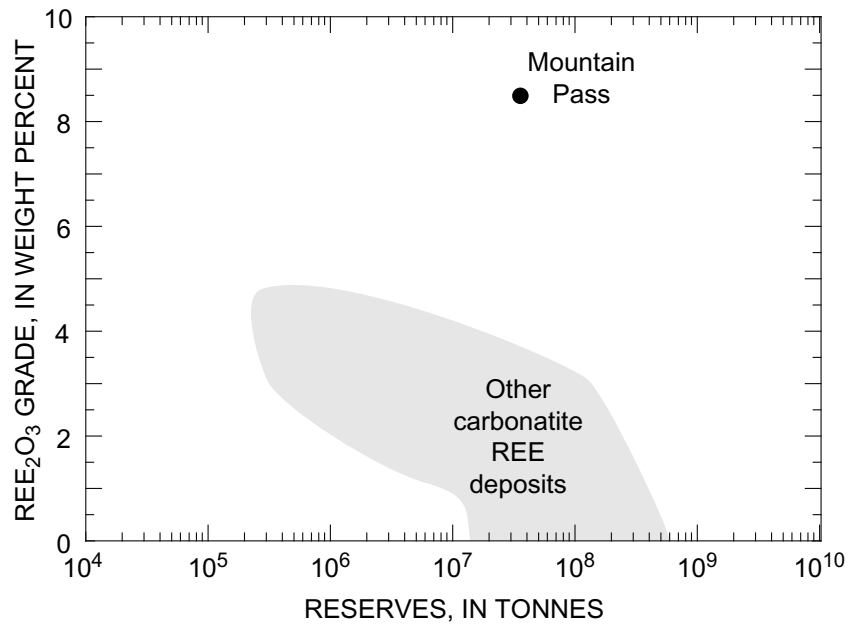


Figure 24. Rare-earth-element (REE) grade and tonnage of the REE deposit at Mountain Pass, Calif. (fig. 2; table 6) compared with 11 other carbonatite REE deposits (D.A. Singer, written commun., 1992).

Table 1. Representative compositions of ultrapotassic rocks and carbonatite, Mountain Pass, Calif.

[LOI, loss on ignition; --, not reported or not determined]

Lithology Sample No. ¹	Shonkinite			Minette OSPS-C	Syenite EM-3	Granite		Carbonatite IGS-40
	C-8	OSPS-A	EM-1			EM-2	EM-4	
Major-element chemistry (weight percent)								
SiO ₂	50.0	47.4	51.5	48.4	54.2	66.9	71.5	16.59
Al ₂ O ₃	11.05	10.6	11.3	10.6	12.1	13.8	13.5	2.1
Fe ₂ O ₃	² 5.95	2.9	3.08	3.4	5.27	2.25	1.97	² 3.28
FeO	--	4.6	4.19	2.7	2.27	.66	1.24	--
MgO	11.4	10.4	7.67	7.	3.67	.73	.6	4.02
CaO	6.72	8.9	4.07	6.9	3.71	1.16	1.30	16.99
Na ₂ O	.56	1.2	1.98	1.3	2.16	3.09	1.45	.12
K ₂ O	8.68	7.	9.06	9.	9.63	8.32	4.42	1.28
TiO ₂	.79	1.6	1.08	2.9	.86	.35	.38	.185
P ₂ O ₅	1.41	2.	1.96	2.4	1.05	.2	.06	.54
MnO	.09	.18	.14	.08	.11	.06	.07	.4
H ₂ O	--	--	.69	--	.45	.27	1.39	--
CO ₂	--	--	.05	--	1.94	.62	.83	18.
F	--	--	1.36	--	.41	.11	.09	.61
LOI	.56	1.1	--	3.2	--	--	--	--
Total ³	98.4	99.6	⁴ 99.3	99.	⁴ 99.	⁴ 99.1	⁴ 99.2	⁵ 99.5
<i>mg</i> ⁶	.82	.76	.71	.73	.53	.37	.30	.75
K ₂ O/Na ₂ O	15.5	5.8	4.6	6.9	4.5	2.7	3.	10.7
Trace-element chemistry (parts per million)								
Cr	575	--	410	--	52.0	11	34.7	--
Ni	--	--	130	--	78	<27	<24	48
Co	--	--	27.2	--	23.7	4.8	6.2	--
Sc	--	--	22.8	--	18.7	5.	10.6	--
Cs	--	--	16.7	--	9.33	4.91	4.94	--
Rb	722	--	572	--	592	439	152	24
Ba	5,600	10,700	5,540	7,400	4,730	2,450	1,300	121,000
Sr	2,300	--	2,130	--	971	440	270	37,200
Th	--	--	302	--	163	183	38.7	202
U	--	--	27	--	14.6	17.5	1.7	210
Zr	--	--	870	--	750	740	190	--
Hf	4.2	--	25.2	--	26.8	18.7	7.35	--
Nb	--	--	28	--	42	40	--	102
Ta	--	--	1.6	--	1.8	2.95	0.23	--
La	255	--	315	--	313	127	79.5	20,700
Ce	564	--	657	--	675	241	155	33,800
Nd	190	--	250	--	290	79	59	8,316
Sm	41.7	--	51	--	60.5	15.5	10.8	517
Eu	9.4	--	10.3	--	12.0	3.05	1.81	86
Tb	2.8	--	3.61	--	4.02	1.35	0.76	⁷ 57
Yb	3.1	--	4.0	--	4.3	2.9	2.4	⁷ 4.1
Lu	.2	--	.53	--	.53	.31	.37	⁷ 81.1
Y	--	--	70	--	45	44	26	110
Eu/Eu* ⁹	.93	--	.82	--	.82	.74	.68	.91
Cl	--	--	120	--	120	240	70	4,000
S	--	--	100	--	1,900	200	<100	34,500

¹Sources of analytical data: C. Crow (1984); IGS, Lister and Cogger (1986); OSPS, Olson and others (1954). All other samples (EM-1 through EM-4) are newly reported; analysts: P.A. Baedeker, D.L. Fey, J. Kent, J.S. Mee, M. Motooka, S.T. Pribble, and D.F. Siems.

²Total iron as Fe₂O₃.

³Totals include oxides of Ba, Sr, Rb, La, Ce, Nd, Cr, and Zr, for samples in which these elements were reported.

⁴Totals for samples EM-1 through EM-4 include F and S with correction for equivalent O.

⁵Total for IGS-40 includes Cl and F with correction for equivalent O; SO₃; and oxides of Ba, Sr, Th, Pb, La, Ce, Pr, Nd, Sm, Eu, Gd, and Y.

⁶*mg* = molar MgO/(MgO+FeO), where weight percent Fe₂O₃/(Fe₂O₃+FeO) = 0.2.

⁷Value is not well determined.

⁸Value is estimated; published value (129 ppm Lu₂O₃) is presumably a misprint.

⁹Eu* = 10^{(2/3 log(Sm)+1/3 log(Tb))}.

Table 2. Ideal formulae of unusual rare earth minerals in carbonatite at Mountain Pass, Calif.

Mineral	Formula ¹
Ancylite	$\text{SrCe}(\text{CO}_3)_2\text{OH}\cdot\text{H}_2\text{O}$
Bastnaesite	$(\text{Ce,La})(\text{CO}_3)\text{F}$
Cerite	$(\text{Ce,Ca})_9(\text{Mg,Fe}^{2+})\text{Si}_7(\text{O,OH,F})_{28}$
Florencite	$\text{CeAl}_3(\text{PO}_4)_2(\text{OH})_6$
Hydroxyl-bastnaesite	$(\text{Ce,La})(\text{CO}_3)(\text{OH,F})$
Parisite	$(\text{Ce,La})_2\text{Ca}(\text{CO}_3)_3\text{F}_2$
Sahamalite ²	$(\text{Mg,Fe})(\text{Ce,La})_2(\text{CO}_3)_4$
Synchisite	$(\text{Ce,La})\text{Ca}(\text{CO}_3)_2\text{F}$

¹From Clark (1984).

²First discovered at Mountain Pass (Jaffe and others, 1953).

Table 3. Batch partial-melting model for incompatible elements in shonkinites at Mountain Pass, Calif. Melt fraction is 0.01 percent.

	Amphibole ¹	Phlogopite ^{2,3}	Clinopyroxene ¹	Rutile ^{2,4}	Apatite ²	D
Th	0.04	0.01	0	0.02	1.4	0.0036
Rb	.20	.25	0.01	0	.01	.0188
Ba	.25	.29	.01	0	.01	.023
Ta	.44	.1	.05	99.5	.03	.276
La	.17	.03	.05	.01	14	.0245
Ce	.26	.03	.1	.01	16	.0332
Sr	.12	.21	.07	0	3	.0192
Nd	.44	.03	.21	.01	20	.0512
P	0	0	0	0	30	.0275
Sm	.76	.03	.26	.01	21	.0703
Hf	.44	.25	.02	4.8	.05	.0432
Ti	.69	.09	.1	30	0	.144
Tb	.83	.04	.27	.02	15	.0692
Yb	.59	.04	.28	.07	9	.0527
Mass fraction of minerals in source rock (percent)						
	Amphibole ⁵	Phlogopite ⁵	Clinopyroxene	Rutile	Apatite	Total ⁶
	4.92	3.40	5.00	0.25	0.09	13.7
Abundance, chondrite normalized⁷						
	Mantle source ⁸	Model magma	Shonkinite ⁹	Abundance ratio, model magma/shonkinite		
Th	19.3	5200	7167	0.73		
Rb	40.7	2150	1634	1.32		
Ba	24.2	1050	803	1.3		
Ta	39.5	143	80	1.79		
La	22.2	900	957	.94		
Ce	19.7	591	657	.9		
Sr	9.62	498	181	2.76		
Nd	11.6	226	397	.57		
P	5.2	189	187	1.01		
Sm	5.78	82.1	251	.33		
Hf	4.44	103	126	.81		
Ti	1.51	10.4	10.5	.99		
Tb	3.26	47.0	69.4	.68		
Yb	1.12	21.2	18.2	1.16		
(La/Yb) _{cn} ¹⁰	20	42	53	.81		

¹From Irving and Frey (1984), McKenzie and O'Nions (1991), and Hawkesworth and others (1993).

²Selected or averaged from numerous published sources, using geometric means and medians rather than arithmetic means.

³Value for Ba from Guo and Green (1990). Regarding Ba and Rb, see text.

⁴Values for Ta and Hf in rutile from Jenner and others (1994). Other values are for ilmenite; see text.

⁵These two variables are related: $[K_2O]_{\text{source}} = x_{\text{phlog}}^s [K_2O]_{\text{phlog}} + x_{\text{amph}}^s [K_2O]_{\text{amph}}$, where the concentration of K₂O in the source rock, in phlogopite, and in amphibole are taken as 0.39, 9.3, and 1.5 percent, respectively (averages from Irving and Frey, 1984; Menzies and others, 1987).

⁶The remaining 86.3 percent of the source rock comprises harzburgitic olivine and orthopyroxene; see text.

⁷Normalizing values (R.N. Thompson, 1982) are chondritic except that values for Rb and P are estimates for primordial or undepleted terrestrial mantle (Sun, 1980).

⁸Geometric means of compositions of eight xenolithic enriched peridotites and pyroxenites, RS1 to RS7 (inclusive), and RS9; RS8, a glimmerite, is excluded (Menzies and others, 1987). Mean K₂O for these samples is 0.39 weight percent.

⁹Sample EM-1 (table 1, figs. 15A, 20A).

¹⁰Chondrite normalized.

Table 4. Analyses of bastnaesite at Mountain Pass, Calif.

[--, not applicable or not calculated]

	Reported ¹	Recalculated, impurity free ²	Ideal bastnaesite ³
Abundances, in weight percent			
	<u>Attributed to bastnaesite</u>		
Ce	27.7	--	--
La+Pr+Nd	31.3	--	--
Ce+La+Pr+Nd	⁴ 59.1	65.35	64.0
CO ₃	25.	⁵ 25.76	27.4
F	6.88	7.61	8.67
	<u>Attributed to impurities</u>		
SiO ₂	4.42	--	--
Ba	1.97	--	--
SO ₄	.74	--	--
Ca	.5	--	--
Mg	.22	--	--
Na+K	.08	.09	--
H ₂ O ⁻	<u>.22</u>	<u>.24</u>	--
Total	99.1	99.1	100
Abundances, in parts per million⁶			
Rb	<10	--	--
Sr	3200	--	--
Zr	<10	--	--
Nb	<10	--	--
Y	>200	--	--

¹Calculated from analysis of impure bastnaesite separate that contains about 5 volume percent quartz and minor amounts of barite and carbonate minerals (Olson and others, 1954, table 7).

²Recalculated free of SiO₂, BaSO₄, CaCO₃, MgCO₃, and BaCO₃.

³Assuming same proportions of La, Ce, Pr, and Nd as bastnaesite samples in table 4; ideal formula is (Ce,La,Nd,Pr)(CO₃)F.

⁴Value is a subtotal.

⁵Value is reduced by amount of CO₃ needed to form CaCO₃ and MgCO₃, as well as to form BaCO₃ from Ba in excess of that required for BaSO₄.

⁶Analyses by energy-dispersive X-ray fluorescence spectrometry; analyst, J. Kent. Sample number 91TT100.

Table 5. Proportions of rare earth elements (REE) and Y in bastnaesite concentrate and average ore from Mountain Pass, Calif.

[All values in weight percent except values in *italic*, which are in parts per million; --, not reported]

	Proportion of REE	
	Bastnaesite concentrate ¹	Average ore ²
La	34	33
Ce	48	49
Pr	4.3	4
Nd	12.4	13
Sm	.81	.5
Eu	.11	.1
Gd	.18	.2
Tb	<i>160</i>	--
Dy	<i>330</i>	--
Ho	<i>52</i>	--
Er	<i>37</i>	--
Tm	<i>8</i>	--
Yb	<i>14</i>	--
Lu	<i>1</i>	--
Y	<i>850</i>	--
Tb+Y	--	.1
Other HREE ³	--	.2
Total	100.0	100.1

¹Recalculated from Neary and Highley (1984).

²From Barnum (1989).

³Heavy rare earth elements.

Table 6. Estimates of proven and probable reserves and grade for the Mountain Pass rare earth element (REE) deposit, Calif.

[--, not reported]

Reserves (10 ⁶ tonnes)	¹ REE ₂ O ₃ grade (weight percent)	Year of estimate	Cut off grade (weight percent)	Reference
28	9	--	5	Barnum, 1989
36	7.67	End 1986	--	Mariano, 1989a
28	8.86	--	--	Mariano, 1989b
29	8.9	1987	5	Castro, 1990, 1991
24.5	--	End 1990	--	J. Landreth, written communication, 1992

¹Rare earth element oxide.

Table 7. Prices of rare earth element oxides from the Mountain Pass deposit, Calif.

[From Molycorp, Inc. Price Schedule, June 1, 1992 (E. Barnum, written communication, 1992)]

Oxide	Purity (weight percent)	Price (\$/kg)
La ₂ O ₃	¹ 99.99	21
CeO ₂	96.0	16
CeO ₂	99.0	23
Pr ₆ O ₁₁	96.0	39
Nd ₂ O ₃	96.0	16
Nd ₂ O ₃	99.9	99
Sm ₂ O ₃	96.0	132
Eu ₂ O ₃	99.99	1,819
Gd ₂ O ₃	¹ 99.99	132
Tb ₄ O ₇	99.9	882
Dy ₂ O ₃	96.0	143
Dy ₂ O ₃	99.0	187
Er ₂ O ₃	98.0	154
Y ₂ O ₃	99.99	121

¹Also available at 99.995% purity.